GEORGIA INSTITUTE OF TECHNOLOGY

OFFICE OF RESEARCH ADMINISTRATION

no action
ack

RESEARCH PROJECT TERMINATION

Date: October 19, 1973

Project Title: "Application of the FInite Difference Method in Seismology to Crust and Upper Mantle Studies"

Project No: G-35-603 (formerly B-3503

Principal Investigator: Dr. L. T. Long

Sponsor: National Science Foundation

Effective Termination Date: October 22, 1973

Clearance of Accounting Charges: charges are clear

patent report
equipment report
Technical report

COPIES TO:

Principal Investigator
School Director
Dean of the College
Director of Research Administration
Associate Controller (2)
Security-Reports-Property Office L
Patent and Inventions Coordinator

Library, Technical Reports Section
Rich Electronic Computer Center
Photographic Laboratory
Terminated Project File No. _____
Other _____

RA-4 (5/70)

GEORGIA INSTITUTE OF TECHNOLOGY
SCHOOL OF GEOPHYSICAL SCIENCES
Atlanta, Georgia 30332
(404) 894-2857

September 30, 1973

NV-1-129-1

National Science Foundation
Washington, D. C. 20550
Attn: Program Director for Geophysics

Subject: Final Technical Letter Report

Principal Investigator: Leland Timothy Long, School of Geophysical Sciences, Georgia Institute of Technology

Grant Number: GA-12391, Starting: April 17, 1969

Title: A Finite Difference Method Applied to Seismic Wave Propagation in Vertically Inhomogeneous Media and Application to Compressional Seismic Arrivals from the Crust and Upper Mantle.

Dear Sir:

This final technical letter report is presented in three parts. Part one is a brief description of the research including results and recommendations. Part two presents scientific collaborators, theses, and talks supported by the grant. Finally, part three presents a detailed technical report on the most significant accomplishment.

NSF support on this grant came at a critical time in the development of the principal investigator and a geophysics program in Geophysical Sciences. The contribution of NSF Support to the goals of the principal investigator and success of the geophysics program now in the School of Geophysical Sciences is greatfully acknowledged.

Respectfully submitted

Dr. Leland Timothy Long
Principal Investigator

LTL:gh

A Finite Difference Method Applied to Seismic Wave Propagation in Vertically Inhomogeneous Media and Application to Compressional Seismic Arrivals from the Crust and Upper Mantle.

Part One: Brief Description of Research

The initial work on the grant was directed toward understanding and testing the basic principles of the finite difference technique in one dimension. At the time of initiation of the research, seismic applications of the finite difference method were few and limited to homogeneous media. The most typical utilization of the finite difference technique was directed at problems in heat flow or similar non-oscillatory phenomenon. Consequently, one-dimensional seismic problems were investigated perhaps longer than warranted. The more intense development of one-dimensional formulations allowed the preliminary evaluation of numerous concepts and computation techniques which were essential to the success of the two-dimensional computations.

The equivalence between the solution of the boundary conditions for a welded contact and the gradient formulation for a sharp gradient was first shown in one dimension. The difficulties and inaccuracies that arise from mixing centered and one-sided differences were also examined. These tests indicated that to avoid unsuspected inaccuracies in the representation of the differential equations, centered difference equations should be used exclusively. The one-dimensional formulation for reflections from a gradient was compared to the theoretical response and found to be accurate to within the accuracy of the difference approximations. The accuracy of the difference approximations, in turn, depended on the space and time increments used showing that the

gradient formulation approached the theoretical solution in the limit of small increments.

Computer programs were written in both real number and integer calculus. Integer calculus yielded approximately a 40 percent reduction in computer time but the programming difficulties in maintaining precision and reducing truncation bias were significant. Consequently, the reduction in computer time was not considered worth the extra programming effort. The results of one-dimensional explicit and implicit finite difference methods were also examined. The usual advantage of the stability of the explicit methods at longer time steps could not be realized in seismic wave simulation because of the time variation of the particle motion. Also, the explicit methods required considerably longer computation times. The implicit methods with filtering effectively do the same computation more economically. In general, the implicit computations required less computer time than expected. The longest two-dimensional elastic media program required six minutes.

A considerable variety of source functions were tested in one dimension. The theoretical impulse response of an elastic media typically exhibits an abrupt initiation and infinite duration or perminant displacement. These features were found to introduce the less accurate higher frequencies or to require larger grids, respectively. By computing the finite difference or filtering the source function, the frequencies could be limited to those easily handled by the difference methods. However, the simplest and best results were obtained with a finite pulse designed to satisfy the frequency limitations of the difference method.

The investigation of boundary conditions for termination of the

grid showed that for each type of boundary an appropriate independent condition was necessary. Perfectly rigid or free surfaces were easily specified from displacement or stress conditions at the boundary. A boundary which generated no reflections could be developed by approximating the wave motion with a Taylor's expansion and theoretically propagating the wave one time step at the boundary. The accuracy depended on the number of terms retained in the approximation as well as the accuracy of the difference equations.

Two-dimensional finite-difference computations were initially applied to a fluid media with a gradient in velocity. The gradient formulation for a fluid is very similar to the formulation for horizontal shear-wave propagation. The results showed the feasibility of studying particle motions near focal points in the media containing a gradient. Also, distinct head waves could be generated with a reasonable amount of computer time. In order to keep the computer storage and computation time at a minimum, a method was developed to move a smaller grid along the area of interest in the wave front.

In an elastic media the exact boundary conditions, where applied to centered difference equations, generally yielded implicit relations which are difficult or time consuming to solve. Hence, in this case, the gradient formulation resulted in a simplification of the computation. The finite difference equations of motion were developed for an arbitrary velocity variation in two dimensions. The validity of the formulation was shown by considering the limit as the thickness of the gradient zone separating two uniform media goes to zero. The results showed that the finite difference methods can give displacements which agree with theoretical data within the error limit determined by the

finite difference grid. Displacement fields showing reflected, compressional and shear waves and all the head waves were generated with a reasonable amount of computer time. Various examples of gradients were computed to test the effect of the gradient on reflected and head waves. Fault cases were computed to show the effect of the faults on the development of the head waves and the diffraction of the waves about the fault.

The specific problem to which the finite difference application was originally directed concerned the development and character of the head wave. More specifically, the research was attempting to determine whether the head wave has the character of the displacement or the displacement potential when a velocity gradient exists at the interface. The finite difference computations indicate that the shape of the head wave corresponds to the displacement. The analysis of Cerveny and Ravindra (1970) indicate that with a gradient, ray theory also predicts a shape similar to the displacement but the mechanism is poorly understood. The head wave with a shape similar to the displacement potential may only exist under ideal conditions.

The finite difference technique for an inhomogeneous media was applied here to the study of head waves. However, the technique is generally applicable to any seismic propagation problem involving irregular velocity structures. The use of transparent boundaries to terminate the grid and thus to minimize computer requirements extends the effective usefulness of the technqiue to the study of selected details of wave motion.

Based on the results and experience of this research the following recommendations are given:

1. The method should be applied more often to seismic problems involving complex velocity distributions.

2. The relations between finite element and finite difference techniques should be examined for possible mixed applications.

3. The theory should be extended to include the effects of attenuation.

4. The theory should be extended to allow evaluation of anisotropic media.

A Finite Difference Method Applied to Seismic Wave Propagation in Vertically Inhomogeneous Media and Application to Compressional Seismic Arrivals from the Crust and Upper Mantle.

Part Two: Collaborators, Thesis and Presentations

At the time of initiation of Grant No. 12391, Geophysical Sciences was a section of the School of Ceramic Engineering with only a few graduate students. The task of finding students capable of this type of work was more difficult than anticipated. Geophysical Sciences is now a school with nearly 30 active graduate students of which at least five are interested in geophysics. Geophysical Sciences has grown significantly and NSF support has contributed to its growth. Nevertheless, for a student to contribute significantly to a program using a difficult technique like finite differences, he should have ability, interest, and sufficient background to understand why the technique is being developed. These qualities, unfortunately, are usually only found in the more advanced graduate students. Geophysical Sciences is now authorized to offer the Ph.D., but it will be awhile before this type of student is attracted to Geophysical Sciences.

The NSF Grant No. 12391 has supported five students over the past four years.

Uday P. Mathur worked for approximately one year on the programming of one-dimensional problems. While supported by this grant he wrote his M.S. thesis titled "Study of the Continental Structure of Southeastern United States by Dispersion of Rayleigh Waves." A condensed version of this thesis was published as: Long, L. T, and Uday P. Mathur. "Southern Appalachian Crustal Structure from the Dispersion

of Rayleigh Waves and Refraction Data." Earthquake Notes, Vol. XLIII, No. 1, 1972.

Frank B. Jones worked for one year on the programming of wave propagation in fluid media. He is currently teaching physics and introductory geophysics at Georgia Southwestern College, Americus, Georgia and intends to continue work toward a Ph.D. in Geophysics. He has installed and maintained a seismic observatory (AMG) on the Georgia Southwestern campus.

J. B. Oliver assisted for one term on the programming and routine analysis of some of the data for the fluid media case. He is currently continuing his studies in Geophysical Sciences.

Nickolas L. Faust assisted for one year in the programming of the wave propagation in the elastic media. He is currently applying his background experience and computing skills to the analysis of ERTS- MSS digital data. He intends to earn a Ph.D. in the field of remote sensing.

Harry E. Denman assisted for about three terms with the analysis and display aspects of the propagation in elastic media. He intends to complete his M.S. degree in early 1974 and work in applied geophysics.

The results of the research have been presented in two talks.

1. L. T. Long, "Finite difference propagation of waves in fluid media with linear velocity gradient." Eastern Section SSA, Penn. State Univ., Oct. 7, 1971

2. L. T. Long, "Finite difference propagation of elastic waves near a velocity discontinuity and gradient,"Western AGU, San Francisco, California, Dec. 7, 1972.

A Finite Difference Method Applied to Seismic Wave Propagation in Vertically Inhomogeneous Media and Application to Compressional Seismic Arrivals from the Crust and Upper Mantle.

Grant No. 12391

Part three: Detailed Technical Results

Part three is a first draft of a proposed publication to present the results of this research. Contemplated revision will largely condense the notation and refine the analysis.

TABLE OF CONTENTS

LIST OF FIGURES

LIST OF FIGURES (concluded)

A STUDY OF THE EFFECTS OF A GRADIENT OR STRUCTURAL IRREGULARITY ON THE GENERATION OF HEAD WAVES; A FINITE DIFFERENCE APPROACH.

Introduction

Refracted waves have been used extensively in earthquake studies, geophysical prospecting and crustal studies (see, for example Musgrave, (1967). The theoretical problems related to the propagation of refracted waves including head waves have been discussed extensively in a number of books and papers (see, for example Brekhovskikh, 1960; Cagniard, 1962; Zvolinskiy, 1965; Cerveny and Ravindra, 1970). Most of these consider only the simplest seismological situation for which closed solutions could be obtained by wave integral methods or approximate solutions by expanded ray methods. The complications in the theory introduced by gradients in velocity or irregularities on the refracting interface have only been investigated by techniques which approximate the wave fronts or ray paths. A complete analytic solution has been possible only for some of the simplest geometrics or limited depth-velocity functions (Cagniard, 1962; Hook, 1965). Approximate solutions for refractions from a gradient in elastic media have been presented using finite layers (Helmberger, 1968; Brekhovskikh, 1960). Hirasawa and Berry (1971) presented solutions for head and reflected waves in a linear transition layer in fluid media in the frequency domain. These results were in agreement with theoretical seismograms generated for approximate elastic media by Fuchs (1968).

Regardless of the theoretical advances, complete theoretical seismograms are available for only simpler cases because general results are quite complicated and simple computational formulas are not available.

To overcome these difficulties, Alterman and Karal (1968) introduced a finite difference equation formulation for a single layered half space with internal source. The finite difference methods possess much greater generality and offer a conceptually simpler approach to the solution of seismic problems in the time domain. Alterman and Karal (1968) show that the finite difference methods give valid results and can be used to obtain complete theoretical seismograms.

The purpose of this paper is to extend the finite difference methods to the study of limited regions of an elastic medium where the physical parameters may be varied arbitrarily. The technique is applied to the generation of refracted, reflected and head waves at a discontinuity perturbed by velocity gradients or structural irregularities.

Most structural problems in seismology can be solved with the measurement of the traveltime of seismic waves through the structure. However the measurement of attenuation or the frequency content of the source requires an understanding of the transmission factors which affect frequency content of the refracted waves. Theoretical studies (for example, Zvolinskiy, 1965) indicate that the head wave should have the character of the source displacement potential and the direct wave the character of the source displacement. Long and Berg (1969) applied this principle to the refracted waves from nuclear explosions and concluded that the head wave was not seen. The major factor contributing to the absence of the head wave with the classical shape of the displacement potential was the existence of a gradient and structural irregularities inferred from traveltime and amplitude measurements.

Evidence for the existence of velocity gradients come from the study

of velocity in materials under pressure, refraction surveys and study of arrival character. Theoretical studies of the pressure dependence of velocity in granite (Birch, 1960) or oceanic crust (Fox et.al., 1973) indicate that an increase in velocity with depth is characteristic of assumed crustal materials. Refraction measurement in Missouri (Stewart, 1968) and in the Western Lake Superior region (Smith et.al., 1966) strongly support the existence of gradients. Helmberger (1968) in synthesizing arrivals from the crust-mantle transition found that arrivals from certain regions in the Bering Sea were represented best by models containing a transition zone.

The explanation for the lack of head waves in regions with velocity gradients (Long and Berg, 1969) is not completely clear. For a slight gradient there should be little distinction between the head and refracted wave. However, as head waves are derived theoretically from second order ray theory the first order terms introduced by the gradients (termed interference head waves by Cerveny and Ravindra, 1970) could dominate the wave motion. These have the character of the displacement since they are first order. The analysis of Hirasawa and Berry (1971) for gradients in a fluid media support the first order character of these waves. The sharp discontinuities approximated with the finite difference method in this study predominantly shows the character of the displacement for the refracted phases and not the displacement potential. By allowing detailed examination of the wave motion along the boundary it is hoped that the finite difference application of this study will add to the understanding of this problem.

Definition of Problem

The finite difference technique is used here to investigate the effects of a gradient or structural irregularity on the generation and propagation of head waves. All problems considered contain essentially two dimensional structures. Because of the distance from the source to the emergent head waves, a two dimensional or cylindrical source is used. At these distances the curvature from a point source would be slight, plane-wave theory would be valid and amplitudes can be converted geometrically from the observed amplitudes for a cylindrical source to expected amplitudes for a point source. The equations of motion are derived in a general form for propagation in a media with a two-dimensional source and two-dimensional inhomogeneties. The use of the general form for inhomogeneous media is valid for smooth or sharp gradients. For SH waves or in a fluid media the sharp gradient is shown to be numerically equivalent to setting up and solving the boundary conditions at the interface between two distinct media. For P-SV motion in elastic media this equivalence may also be true but the equation can not be solved explicity. The first case investigated is a simple sharp horizontal discontinuity. It serves as a check on the validity and accuracy of the numerical method since its solution is known approximately. Then structures in which the gradients are modified above or below the discontinuity are investigated for the effects on the amplitudes of the head wave and converted waves. Finally the effects of a vertical step in the horizontal discontinuity are investigated.

Equations of Motion

For motion in a perfectly-elastic, inhomogeneous, isotropic

medium the equations of motion can be written in the form (Sokolnikoff, 1964, pg. 343)

$$g^{jk}\tau_{ij,k} = \rho \frac{\partial^2 U_i}{\partial t^2} \tag{1}$$

where τ_{ij} is the stress tensor, g^{jk} the contravariant fundamental tensor and $\rho\partial^2 U_i/\partial t^2$ the inertial force. The subscript notation ",j" represents covariant differentiation. The stress is expressed in terms of the displacements U_i by substituting the strain tensor

$$\varepsilon_{ij} = \tfrac{1}{2} (U_{i,j} + U_{j,i}) \tag{2}$$

and the stress-strain relations

$$\tau_{ij} = \lambda g^{ij} \varepsilon_{ij} g_{ij} + 2\mu\varepsilon_{jk} \tag{3}$$

into the equations of motion. By considering that the Lame' constants λ and μ are two-dimensional functions of position and that the source is also two-dimensional, the equation of motion in orthogonal cartesian coordinates takes the form:

$$\frac{\partial^2 U_1}{\partial t^2} = \alpha^2 \frac{\partial^2 U_1}{\partial x_1^2} + (\alpha^2 - \beta^2) \frac{\partial^2 U_3}{\partial x_1 \partial x_3} + \beta^2 \frac{\partial^2 U_1}{\partial x_3^2} \tag{4}$$

$$+ R_{13} + S_{31}$$

$$\frac{\partial^2 U_2}{\partial t^2} = \beta^2 \left[\frac{\partial^2 U_2}{\partial x_1^2} + \frac{\partial^2 U_2}{\partial x_3^2}\right] + \frac{1}{\rho}\frac{\partial(\rho\beta^2)}{\partial x_1}\frac{\partial U_2}{\partial x_1} + \frac{1}{\rho}\frac{\partial(\rho\beta^2)}{\partial x_3}\frac{\partial U_2}{\partial x_3} \tag{5}$$

$$\frac{\partial^2 U_3}{\partial t^2} = \alpha^2 \frac{\partial^2 U_3}{\partial x_3^2} + (\alpha^2-\beta^2)\frac{\partial^2 U_1}{\partial x_1 \partial x_3} + \beta^2 \frac{\partial^2 U_3}{\partial x_1^2} + S_{13} + R_{31} \tag{6}$$

where $R_{ij} = \frac{1}{\rho}\frac{\partial(\rho\alpha^2)}{\partial x_i}\frac{\partial U_i}{\partial x_i} + \frac{1}{\rho}\frac{\partial(\rho\alpha^2 - \rho\beta^2)}{\partial x_i}\frac{\partial U_j}{\partial x_i}$

$$S_{ij} = \frac{1}{\rho}\frac{\partial(\rho\beta^2)}{\partial x_i}\left[\frac{\partial U_i}{\partial x_j} + \frac{\partial U_j}{\partial x_i}\right]$$

$\alpha = \left(\frac{\lambda+2\mu}{\rho}\right)^{\frac{1}{2}} = \alpha(x_1, x_3) =$ compressional wave velocity

$\beta = \left(\frac{\mu}{\rho}\right)^{\frac{1}{2}} = \beta(x_1, x_3) =$ shear wave velocity

$\rho = \rho(x_1, x_3) =$ density

Equation 5, representing SH-wave propagation can be simplified further by the transformation

$$y = \int_0^z \frac{1}{\rho\beta^2}\, dx_3$$

provided the velocity varies in one direction only. Application of the transformation gives the simple form:

$$\frac{\partial^2 U_2}{\partial t^2} = \beta^2 \frac{\partial^2 U_2}{\partial x_1^2} + \frac{1}{\rho^2 \beta^2} \frac{\partial^2 U_2}{\partial y^2} . \tag{5a}$$

Finite Difference Approximation

For finite difference computation the partial derivatives in the equation of motion are approximated by centered difference equations. The general form for the difference equations with error terms and arbitrary increments can be derived from a Taylor's Expansion.

$$F(z) = F(z_o) + (z-z_o)\, F'(z_o) + \frac{1}{2!}(z-z_o)^2 F''(z_o) + \ldots$$

$$\ldots + \frac{1}{n!}(z-z_o)^n F^n(z_o) + \ldots \tag{7}$$

where $F'(=) \frac{\partial f}{\partial z}$, $F''(=) \frac{\partial^2 f}{\partial z^2}$ etc.

By evaluating Taylor's expansion for $z = z_o + h_1$, and $z = z_o - h_2$, two expressions are obtained from which $F'(z)$ and $F''(z)$ can be solved for in terms of $F(z)$ and higher order derivatives. These equations are

$$F(z_o+h_1) = F(z_o) + F'(z_o)(h_1) + \ldots + \frac{F^n(z_o)}{n!} (h_1)^n \tag{8}$$

$$F(z_o-h_2) = F(z_o) + F'(z_o)\,(-h_2) + \ldots + \frac{F^n(z_o)}{n!} (-h_2)^n \tag{9}$$

By multiplying equation (8) by h_2 and equation (9) by h_1 and adding, the first derivative term is eliminated and an expression for the second derivative is obtained for arbitrary increments,

$$\frac{h_2F(z_o+h_1) - (h_2+h_1)\,F(z_o) + h_1F(z_o-h_2)}{((h_2 + h_1)/2)\,h_1h_2} = F''(z_o) + \sum_{n=3}^{\infty} \frac{2(h_1^{n-1} + (-1)^n h_2^{n-1})F^n(z_o)}{n!\,(h_2+h_1)} \tag{10}$$

which for equal increments, $h_1 = h_2$, reduces to

$$\frac{F(z_o+h) - 2F(z_o) + F(z_o-h)}{h^2} = F''(z) + \sum_{n=2}^{\infty} \frac{h^{2n-2}F^{2n}(z_o)}{(2n)!} \tag{11}$$

By multiplying equation (8) by h_2^2 and equation (9) by h_1^2 and substracting, the second derivative term is eliminated and an expression for the first derivative is obtained for arbitrary increments,

$$\frac{h_1^2\,F(z_o-h_2) - h_2^2\,F(z_o+h_1) - (h_1^2-h_2^2)F(z_o)}{h_1h_2(h_2+h_1)} = -F'(z_o) - \sum_{n=2}^{\infty} \frac{h_1h_2(h_1^{n-2} - (-1)^n h_2^{n-2})\,F^n(z_o)}{(h_2+h_1)n!} \tag{12}$$

which for equal increments, $h_1 = h_2 = h$, reduces to

$$\frac{F(z_o-h) - F(z_o+h)}{2h} = -F'(z_o) - \sum_{n=2}^{\infty} \frac{h^{2n-2}F^{2n-1}}{2\,(2n-1)!} \tag{13}$$

For a two-dimensional equation of motion, a finite difference approximation to the mixed partial derivative is also needed. It can be derived from equation (13) by substituting F (x,z) for F (z) evaluated for z_o and differentiating by x.

$$\frac{\partial}{\partial x}\frac{(F(x,z_o-h) - F(x,z_o+h))}{2h} = -\frac{\partial}{\partial x}\frac{\partial F(x,z_o)}{\partial z} - \sum_{n=2}^{\infty} \frac{h^{2n-2}}{2(2n-1)!} \tag{14}$$

$$\frac{\partial}{\partial x}\frac{\partial^{2n-1}F(x,z_o)}{\partial z^{2h-1}}$$

the x derivatives are then approximated according to equation (13) and substituted into equation (14). With elimination of products of remainder terms these reduce to

$$\frac{\partial^2 F(x_o,z_o)}{\partial y \partial z} = \frac{(F(x_o-h,z_o-h) - F(x_o+h,z_o-h) - F(x_o-h,z_o+h) + F(x_o+h,z_o+h)}{4h^2}$$

$$+ \sum_{n=2}^{\infty} \frac{h^{2n-2}}{2(2n-1)!}\left[\frac{\partial^{2n-1}}{\partial y^{2n-1}}\frac{\partial}{\partial z} F(x_o,z_o) + \frac{\partial}{\partial y}\frac{\partial^{2n-1}}{\partial z^{2n-1}} F(x_o,z_o)\right] \tag{15}$$

If the remainder terms are eliminated then the centered differences can be used to define difference operators (δ) such that

$$\frac{\partial F(x,z)}{\partial x} \simeq \frac{\delta_x F}{2h}$$

$$\frac{\partial^2 F(x,z)}{\partial z^2} \simeq \frac{\delta_{zz} F}{h^2} \tag{16}$$

$$\frac{\partial^2 F(x,z)}{\partial x \partial z} \simeq \frac{\delta_{xz} F}{4h^2}.$$

The difference operators will simplify the writing of the difference equations.

The centered difference equations (11), (13) and (15) are correct to second order since the remainder terms start with terms involving h^2 or higher powers of h

Finite Difference Equations of Motion

In formulating the finite difference form of the equations of motion the centered differences are used exclusively. Experience has shown that mixing centered and one-sided difference equations do not work well. The reason is that they refer to different positions in the media and can thus introduce unanticipated and unwanted boundary conditions. Mixed difference equations may, in effect, not represent the differential equations being approximated.

Because the problems investigated here limit the finite difference application to a portion of the total media, even increments in space and time are used exclusively. Also the P and S waves simulated maintain their basic character and frequency content through out the media so that the same increment is necessary for consistancy in the accuracy of the finite difference application. This is significantly different from the surface-wave problem where high frequencies are limited to shallow depth and an expanded grid can be used at greater depths. (Boore, 1970).

In order to write the finite difference equations the displacements and material parameters are written in terms of their values at indexed points on an incremented grid in space and time. Thus, at the points $t = p\Delta t$, $x_1 = m\Delta x_1$ and $x_3 = n\Delta x_3$ where p, m and n are integers, the displacements and material parameters have the values

$$U_1(x_1,x_3,t) = U_1\ (m\Delta x_1, n\Delta x_3, p\Delta t) = A^p_{mn}$$

$$U_2(x_1,x_3,t) = U_2\ (m\Delta x_1, n\Delta x_3, p\Delta t) = U^p_{mn}$$

$$U_3(x_1,x_3,t) = U_3\ (m\Delta x_1, n\Delta x_3, p\Delta t) = B^p_{mn}$$

$$\alpha(x_1,x_3) = \alpha(m\Delta x_1, n\Delta x_3) = \alpha_{mn} \tag{17}$$

$$\beta(x_1,x_3) = \beta(m\Delta x_1, n\Delta x_3) = \beta_{mn}$$

$$\rho(x_1,x_3) = \rho(m\Delta x_1, n\Delta x_3) = \rho_{mn}$$

The difference operators can be written in the form

$$\delta_m, \delta_n, \delta_{mm}, \delta_{nn} \text{ and } \delta_{mn}$$

where, for example

$$\delta_{mm}A^p = A^p_{m-1,n} - 2A^p_{mn} + A^p_{m-1,n} \tag{18}$$

On A and the material parameters the subscript (mn) which designates the position in space is omitted where not needed.

After substitution of the centered difference formula, the equations of motion assume an explicit form in which successive values of particle motion are found directly from values at the previous two time increments. Thus, when $\Delta x_1 = \Delta x_3$ the equations are,

$$\begin{aligned} A^{p+1} = {} & 2A^p - A^{p-1} + \left(\frac{\Delta t}{\Delta x}\right)^2 \Bigg[\alpha^2 \delta_{mm} A^p + \left(\frac{\alpha^2-\beta^2}{4}\right)\delta_{mm} B^p \\ & + \beta^2 \delta_{nn} A^p + \frac{1}{4\rho} \Big\{ \delta_m(\rho\alpha^2)\ \delta_m A^p + \delta_m(\rho\alpha^2 - 2\rho\beta^2) \\ & \delta_n B^p + \delta_n(\rho\beta^2)\ (\delta_m B^p + \delta_n A^p) \Big\} \Bigg] \end{aligned} \tag{19}$$

$$B^{p+1} = 2B^p - B^{p-1} + \left(\frac{\Delta t}{\Delta x}\right)^2 \left[\alpha^2 \delta_{nn} B^p + \left(\frac{\alpha^2-\beta^2}{4}\right)\delta_{mm} A^p \right.$$

$$\left. + \beta^2 \delta_{mm} B^p + \frac{1}{4\rho} \left((\delta_m(\rho\beta^2)\ (\delta_n A^p + \delta_m B^p) + \delta_n(\rho\alpha^2)\delta_n B^p \right.\right. \qquad (20)$$

$$\left.\left. + \delta_n(\rho\alpha^2 - 2\rho\beta^2)\ \delta_m A^p \right) \right]$$

$$U^{p+1} = 2U^p - U^{p-1} + \left(\beta\frac{\Delta t}{\Delta x}\right)^2 \left[\delta_{mm} U^p + \delta_{nn} U^p + \frac{1}{4\rho\beta^2} \cdot \right. \qquad (21)$$

$$\left. \left(\delta_m(\rho\beta^2)\delta_m U^p + \delta_n(\rho\beta^2)\ \delta_n U^p \right) \right]$$

Boundary conditions

The formulation of the boundary conditions generally prove to be the most difficult aspect of the finite difference application. For each value which falls outside the grid an independent boundary condition is needed. In general it is necessary to set-up factitious grid points one increment beyond the propagation grid and use the boundary conditions to solve for the appropriate values on the false line. The use of centered difference equations becomes important in boundary formulation since otherwise the effective position of the boundary might not coincide in the two media. The use of both one sided and centered difference equations for the stress continuity conditions at the free surface or an internal surface in an elastic media would place the tangential and normal stress boundary conditions at different planes in the media. Results from this questionable type of formulism may be stable but could be slightly in error. The magnitude of the error would depend on the magnitude of the velocity contrast.

The appropriate application of centered difference equations to a free surface in elastic media is described by Munasinghe and Farnell (1973). However, even though a free surface is not used in this investigation it serves to illustrate the relation between the gradient formulation and a formulation involving solution of boundary conditions. If we assume the velocity and density to be zero ($\rho_{mn} = 0, \alpha_{mn} = 0$, $n < 1$) above the free surface then, at $n = 0$ the finite difference equations reduce to the remainder terms R_{ij} and S_{ij} in their finite difference form.

For a horizontal surface,

$$0 = \frac{1}{4}\left(\frac{\Delta t}{\Delta x}\right)^2 \delta_n(\rho\beta^2)\ (\delta_m B^p + \delta_n A^p)$$

$$0 = \frac{1}{4}\left(\frac{\Delta t}{\Delta x}\right)^2 \rho_{m1}\beta^2_{m1}\ (\delta_m B^p_{mo} + \delta_n A^p_{mo}) \qquad (22)$$

and

$$0 = \frac{1}{4}\left(\frac{\Delta t}{\Delta x}\right)^2 \left[\delta(\rho\alpha^2)\delta_n B^p + \delta_n(\rho\alpha^2 - 2\rho\beta^2)\ \delta_m A^p\right]$$

$$0 = \frac{1}{4}\left(\frac{\Delta t}{\Delta x}\right)^2 \left[\rho_{m1}\alpha^2_{m1}\ \delta_n B^p_{mo} + (\rho_{m1}\alpha^2_{m1} - 2\rho_{m1}\beta^2_{m1})\delta_m A^p_{mo}\right] \qquad (23)$$

However, by comparison with equations (3), equations (22) and (23) represent the boundary conditions for tangential and normal stress at a free surface. These conditions depend on the ratio of shear to compressional velocities, not the magnitude of the velocities, and allow computations of the A and B values on the factitious grid points above the computation grid. In the finite difference formulation for inhomogeneous media (equations 19, 20), remainder terms will exist at the free surface. Otherwise the equations will be identical to the difference equations for homogeneous media where the media is homogen-

eous. The remainder terms thus have the effect of a velocity gradient over one grid point at the free surface. Because it is a sharp gradient, however, it would effect only the high frequencies, which, for reasons of accuracy, should not be present.

The relation between the gradient formulation and the formulation obtained by solving the boundary conditions for two homogeneous media is similar to the smoothing effect observed at the free surface. For SH waves or fluid media (equation 21) the boundary conditions allow an exact solution for values on the factitious lines above and below a horizontal interface. By adding the finite difference expressions evaluated for the upper and lower media, and then substituting the values for the two unknown points on the factitious lines from the stress condition at the boundary, the following equation for SH waves results:

$$U^{p+1} = 2U^{p} - U^{p-1} + \left(\frac{\mu_1+\mu_2}{\rho_1+\rho_2}\right)\left(\frac{\Delta t}{\Delta x}\right)^2 \left[\delta_{mm}U^{p} + \delta_{nn}U^{p}\right] + \frac{1}{2}\,\frac{(\mu_1-\mu_2)}{(\mu_1+\mu_2)}\,(\delta_{n}U^{p}) \tag{24}$$

where

μ_1 = shear modulus of upper media

ρ_1 = density of upper media

μ_2 = shear modulus of lower media

ρ_2 = density of lower media

At the boundary, equation (24) differs from the gradient formulation with mean values of the elastic constants at the boundary, equation (21), by a factor of two in the remainder term. However, the

gradient formulation also adds a remainder term one step above and below the boundary. The sum of these terms is equal to the remainder term in equation (24).

The effect of the gradient formulation is to spread the boundary out over three grid points. By applying the gradient formulation to a simple step change in elastic constants the boundary is spread out over only two grid points. Again the sum of the remainder terms are equal to the remainder in equation 24. The differences in the formulations would only effect the shorter wavelengths.

An analogous comparison of the gradient formulation with the boundary value formulation is more difficult for P-SV wave propagation in elastic media. At the boundary the finite difference equations become implicit and it is necessary to solve for all the values on the factitious lines simultaneously. In the simplest case consisting of three grid points in width with rigid boundaries there are two sets of six simultaneous equations. Although the algebraic equations were not solved exactly, a numerical test showed the equivalence of the boundary value formulation to the gradient formulation used at the boundary with mean values of the elastic constants and twice the remainder term. In the investigation here of the generation of head waves a correct formulation for the boundary value condition was necessary because of the sensitivity of the head wave to velocity gradients near the boundary.

In addition to the physical boundaries associated with the velocity structure of the media, artificial boundaries are introduced by the constraints in computer storage and reasonable computing time. In the cases investigated here the grid is limited to the region of interest

by moving the grid with the wave and utilizing transparent boundaries. Transparent boundaries allow termination of the grid by assuming propagation in one direction and thus do not allow reflections. Previous investigations (Alterman and Karal, 1968; Boore, 1970) either ignored the reflected phases or used a modified grid to extend the net to a distance where reflected phases would not interfere with phases of interest. Neither of these techniques could be utilized in this investigation.

The structures investigated here are primarily perturbations of horizontal interface between two homogeneous media. Hence the grid needed only to be shifted horizontally to follow the interaction of the incident wave with the interface. The vertical boundary in front of the waves was constrained to zero since, in a moving grid, the waves never reach this edge. The vertical boundary at the source was constrained by symetry about the vertical axis. Hence the standard finite difference equations are applied with

$$A^p_{1,n} = - A^p_{-1,n} \qquad B^p_{1,n} = B^p_{-1,n} \tag{25}$$

After an initial time period required to propagate the major portion of the wave into the grid, the grid is shifted with the wave along the interface and the boundary at the origin is left behind.

For the bottom and top boundaries the same transparent boundary condition was applied. However, at the top the incident pulse was removed before computing the transparent boundary values. The independent conditions necessary to terminate a finite difference grid are supplied by assuming that the existing waves near the boundary propagate in the direction of their maximum slope with the appropriate shear

or compressional wave velocity. Hence it is necessary to transform the horizontal and vertical displacements into dilatation and rotation. Also, to assure complete separation the media near the transparent boundary was assumed to be homogeneous. The transformation to dilatation and rotation is effected by writing the differential equations in finite difference form.

$$\Delta = \frac{1}{2}\left(\frac{\partial U_1}{\partial x_1} + \frac{\partial U_3}{\partial x_3}\right)$$
$$\Theta = \frac{1}{2}\left(\frac{\partial U_3}{\partial x_1} - \frac{\partial U_1}{\partial x_3}\right) \qquad (26)$$

$$\Delta^p = \frac{1}{4\Delta x}\left(\delta_m A^p + \delta_n B^p\right)$$
$$\Theta^p = \frac{1}{4\Delta x}\left(\delta_m B^p - \delta_n A^p\right) \qquad (27)$$

Equations (27) are used to compute dilatation and rotation at the second and third grid points from the boundary at time p. The displacements A and B, can be computed for all points except on the boundary for time p+1, the next time step, from the standard explicit finite difference equations of motion for interval points. The values of Δ and Θ at the grid points adjacent to the boundary are then computed for the next time step by theoretically propagating the waves. Equations (27) can then be used at p+1 to solve for the A and B values on the boundary.

In order to propagate the rotational and dilatational waves, the

maximum (i.e. normal) gradients are computed from the relations

$$\frac{\partial \Delta}{\partial n} = \left[\left(\frac{\partial \Delta}{\partial x_1}\right)^2 + \left(\frac{\partial \Delta}{\partial x_3}\right)^2 \right]^{\frac{1}{2}} \tag{28}$$

$$\frac{\partial \Theta}{\partial n} = \left[\left(\frac{\partial \Theta}{\partial x_1}\right)^2 + \left(\frac{\partial \Theta}{\partial x_3}\right)^2 \right]^{\frac{1}{2}} \tag{29}$$

Propagation is then assumed to be in the direction of the maximum gradient and the new values can be written:

$$\Delta^{p+1}_{m,n} = \Delta^{p}_{m,n} + \alpha\Delta t \left(\frac{\partial \Delta}{\partial n}\right) \text{SGN} \left(\Delta^{p}_{m,n-1} - \Delta^{p}_{mn}\right) \tag{30}$$

$$\Theta^{p+1}_{mn} = \Theta^{p}_{mn} + \beta\Delta t \left(\frac{\partial \Theta}{\partial n}\right) \text{SGN} \left(\Theta^{p}_{m,n-1} - \Theta^{p}_{mn}\right)$$

Equations (30) represent a plane wave approximation to the wave at the boundary and give results good to eight percent or better depending on the azmuth of the incident wave and amplitudes of higher derivative components in the wave. Their asymetry, perhaps, contributes to the azimuthal variations in efficiency of this first order approximation. However, the predominent direction of propagation was in the positive x_1 direction and the one sided approximations with bias toward the

negative x_1 direction were considered appropriate for these waves. The eight percent was adequate for the investigations here considering the added computer time required for a higher order approximation in two dimensions. A second order approximation in one dimension is good to better than one percent, or nearly as good as the finite difference approximations at the shorter wavelengths.

Source Function

A solution of the wave equation representing compressional waves propagating cylindrically outward from a line source may be written (Ewing, et.al., 1957, pg. 36) as:

$$\phi_o = i\pi \, e^{i\omega t} \, H_o^{(2)}\left(\frac{\omega R}{\alpha}\right) \tag{31}$$

where $H_o^{(2)}$ is a Hankel function of second kind of zero order and $R^2 = x_1^2 + x_2^2$ is the radial distance from the line source. Where $\left|\frac{\omega R}{\alpha}\right|$ is large,

$$H_o^{(2)}\left(\frac{\omega R}{\alpha}\right) \simeq \frac{2i\alpha}{\pi\omega R} \, e^{-\left(\frac{i\omega R}{\alpha}\right)} \tag{32}$$

Where greater precision is required, higher order terms in the series approximation (Sommerfeld, 1964, p.117)

$$H_o^{(2)}\left(\frac{\omega R}{\alpha}\right) = \frac{2i\alpha}{\pi\omega R} \, e^{-\left(\frac{i\omega R}{\alpha}\right)} \left[1 - \frac{\alpha}{8i\omega R} + \right] \tag{33}$$

can be included. The equation for the potential can then be written:

$$\phi_o(\omega) = A(w) \, \frac{1}{R^{\frac{1}{2}}} \, e^{i\omega\left(t - \frac{R}{\alpha}\right)} \left[1 - \frac{\alpha}{8i\omega R} + \right] \tag{34}$$

where $A(\omega)$ can be considered the spectra of the first order approximation. By comparison with the inverse Fourier transform with respect to ω it can be shown that the general solution to the wave equation for cylindrical propagation in the time domain takes the form

$$\phi = \frac{F(\tau)}{R^{\frac{1}{2}}} \left[1 - \frac{\alpha}{8R} \int^{\tau} F(t')\, dt' + - - - \right. \tag{35}$$

For the cases investigated here the first order approximation was used since the regions of interest were sufficiently removed from the source and $\omega R/\alpha$ was large.

The choice of the function $F(\tau)$ requires consideration of the limitations of the grid and finite difference technique. For the finite difference approximations to give a genuine solution representative of the input function, the first and second derivative of the displacements must be continuous. Hence, the problem must be properly posed in the sense that the input function can contain only frequencies or geometries which can be accurately handled by the finite difference scheme. Also, to resolve phases on the finite difference seismograms the source function should be finite in length and not introduce a net displacement. The potential function chosen is the linear combination of two cosine functions.

$$\phi(\tau) = \frac{F(\tau)}{R^{\frac{1}{2}}} = \begin{cases} (\mathrm{Cos}(2\pi ft) - 0.25\mathrm{Cos}(4\pi ft) - 0.75)/R^{\frac{1}{2}} \\ \\ 0.0, \quad |f\tau| > 1.0 \end{cases} \tag{36}$$

where f is the frequency.

The displacement for the top surface was computed from the relation:

$$U = -\frac{\partial}{\partial R}(F(\tau)/R^{\frac{1}{2}}) = \frac{F(\tau)}{2R^{3/2}} + \frac{2\pi f}{\alpha R^{\frac{1}{2}}} \frac{\partial F(\tau)}{\partial \tau} \tag{37}$$

Its first and second derivative are continuous as can be seen in Figure 1. The length of the pulse can be controlled by the frequency. In the first order approximation it shows no net displacement so that phases can easily be identified on the artificial seismograms and displacement plots.

Others (e.g. Alterman and Karal, 1968) have utilized nth order finite differences of nth order polynomials or other appropriate functions to achieve smooth higher order derivatives. These source functions, however, generally show a sharp front edge and a net displacement. Alterman and Loewenthal (1970) used a zero frequency filter to remove the net displacement. The abrupt initiation is a result of higher amplitudes in the higher frequencies. These sources do provide a single peak for the displacement which helps in identifying phases, but at the cost of near discontinuities in the second derivatives.

In contrast the displacement and dilatation or rotation for the source used here have two or three maxima respectively.

Consistency

By the equivalence theorem, stability by the Von Neumann condition or other condition is a necessary and sufficient condition that the finite difference equation be a convergent approximation to the true solution provided (1) the initial value problem is properly posed and provided (2) the finite difference approximation satisfies the consistency condition. A properly posed pro-

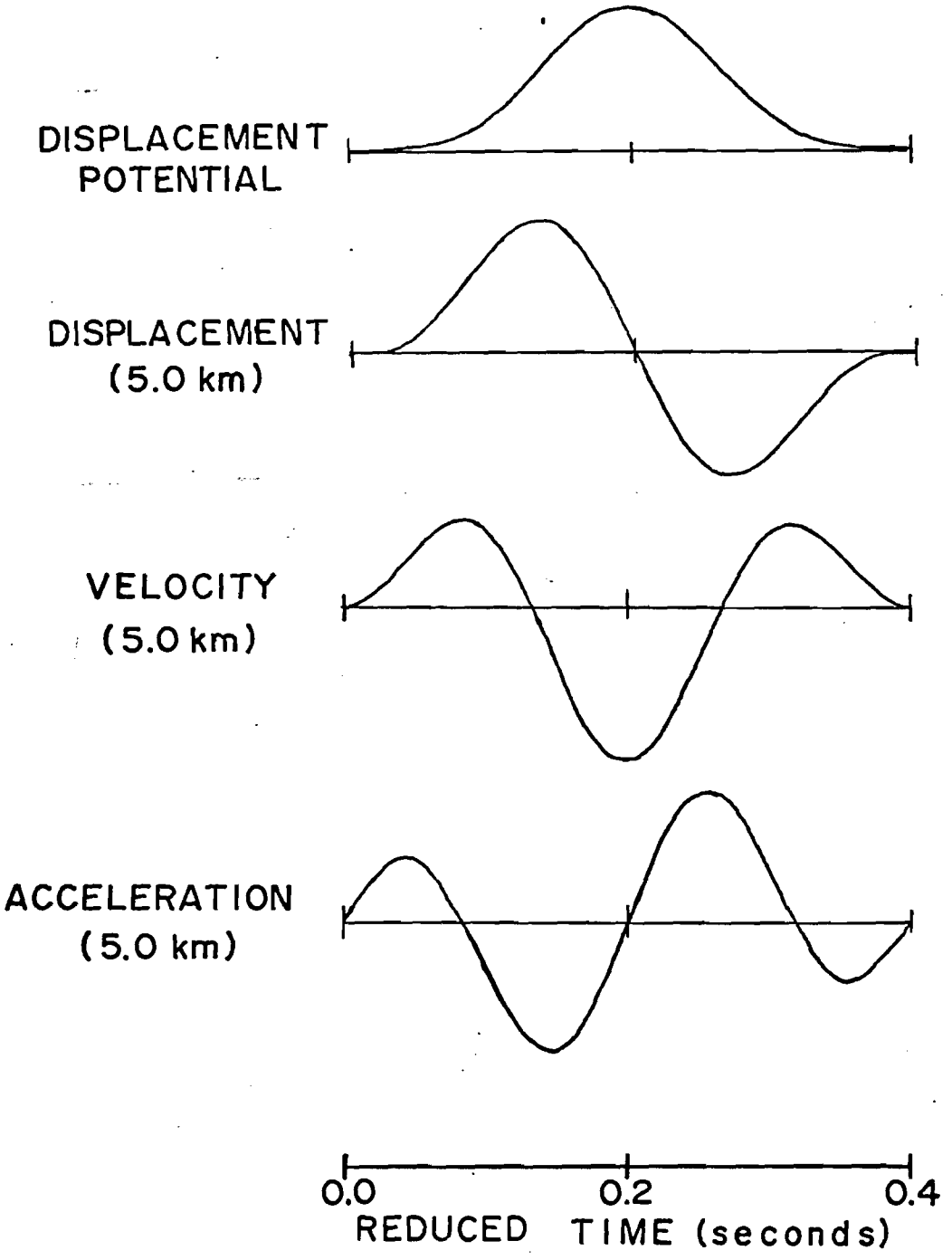

Figure 1. Displacement potential and displacement at 5.0 kilometers for the source used in finite difference computations.

blem requires that the source be chosen to fit the constraints of the finite difference scheme. This was discussed in the previous section.

To verify the consistency condition, the differential operators have to be compared to their finite difference approximation. This amounts to evaluating the remainder terms in the Taylor's series approximation to the differential operators (equations 11, 13, 15). Figure 2 shows the maximum values of the error terms evaluated for a unit amplitude Sine function versus the ratio of grid increment to wave length. The lowest shear wave velocity used (β = 2.23 km/sec) in this study is thus at most in error by about 5 percent with 0.1 kilometer space increments and a period of 0.4 seconds. Thus the consistency requirement is satisfied to 5 percent precision provided $\beta > 2.23$. All longer wave lengths or equivalently higher velocities would be proportionally more precise. Attempts to use velocities lower than 2 km/sec (space increment of 0.1 and period 0.4 seconds) led to erroneous results and in general caused abnormally large reflections from these low velocity regions. The abnormally large reflections were most noticeable where the velocity contrast approaches the limit of stability for the higher velocity P-waves. Accuracy is limited at the longer wavelengths by truncation in the computer. However, the one percent precision level for single precision computer programming (eight significant digits) implies a wavelength of nearly 5000 points and the maximum number of points used in this study was about 100 points.

Stability

In the inhomogeneous portions of the grid, the analysis of

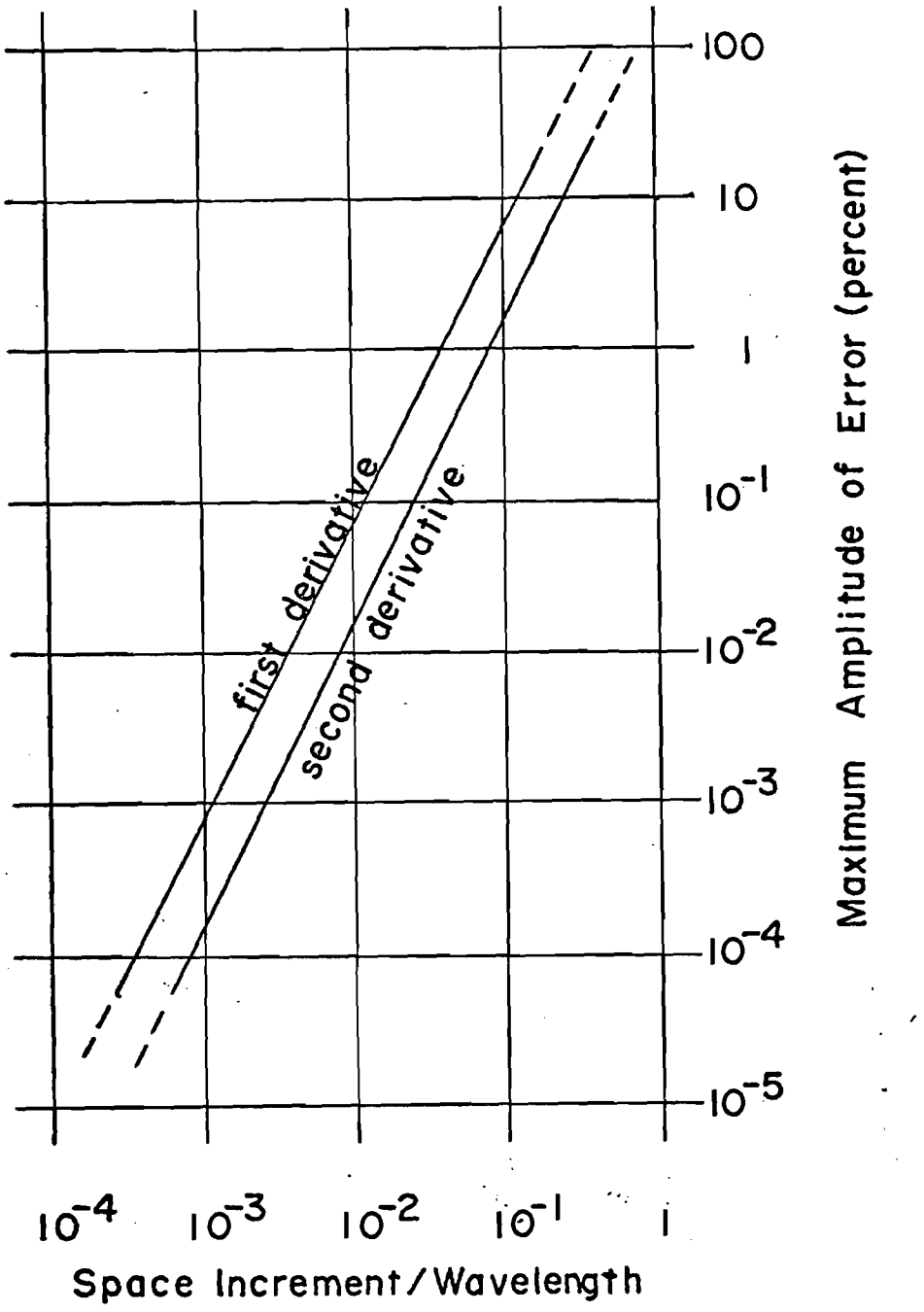

Figure 2. Relation between space increment, wavelength and maximum error of finite difference approximations.

stability must include the effects of the gradients of the elastic parameters. The general procedure in determining stability is to derive the amplification matrix by computing the Fourier transform of the difference equations and by finding estimates for the bounds of its powers (Lax and Richtmyer, 1956). Derivation of the amplification matrix requires that the finite difference equations (equations 19,21) be written in terms of a single time step rather than the two time steps obtained in the difference approximation to the second time derivative. By defining the difference operator δ_p^1 with the equation

$$\delta_p^1 A_{mn}^p = A_{mn}^{p+1} - A_{mn}^p \tag{38}$$

and defining the new quantities R_{mn}^p and S_{mn}^p with the relation

$$\begin{bmatrix} R_{mn}^{p+1} \\ S_{mn}^{p+1} \end{bmatrix} = \frac{1}{\Delta t} \begin{bmatrix} \delta_p^1 A_{mn}^p \\ \delta_p^1 B_{mn}^p \end{bmatrix} = \frac{1}{\Delta t} \begin{bmatrix} A_{mn}^{p+1} \\ B_{mn}^{p+1} \end{bmatrix} - \frac{1}{\Delta t} \begin{bmatrix} A_{mn}^p \\ B_{mn}^p \end{bmatrix} \tag{39}$$

it follows directly that

$$\frac{1}{\Delta t} \begin{bmatrix} \delta_p^1 R_{mn}^p \\ \delta_p^1 S_{mn}^p \end{bmatrix} = \frac{1}{\Delta t} \begin{bmatrix} R_{mn}^{p+1} \\ S_{mn}^{p+1} \end{bmatrix} - \frac{1}{\Delta t} \begin{bmatrix} R_{mn}^p \\ S_{mn}^p \end{bmatrix} = \frac{1}{\Delta t^2} \begin{bmatrix} \delta_{pp} A_{mn}^p \\ \delta_{pp} B_{mn}^p \end{bmatrix}. \tag{40}$$

Thus, by use of equation (40), the finite difference equations of motion for P-SV waves can be written in the form of two implicit finite difference equations which require only a single previous time step. Hence, in matrix form the equations of motion are

$$\frac{1}{\Delta x^2}\begin{bmatrix} D_{11} & D_{12} \\ D_{21} & D_{22} \end{bmatrix}\begin{bmatrix} A^p_{mn} \\ B^p_{mn} \end{bmatrix} + \frac{1}{\Delta t}\begin{bmatrix} R^p_{mn} \\ S^p_{mn} \end{bmatrix} = \frac{1}{\Delta t}\begin{bmatrix} R^{p+1}_{mn} \\ S^{p+1}_{mn} \end{bmatrix}$$

and

$$\frac{1}{\Delta t}\begin{bmatrix} A^p_{mn} \\ B^p_{mn} \end{bmatrix} = -\begin{bmatrix} R^{p+1}_{mn} \\ S^{p+1}_{mn} \end{bmatrix} + \frac{1}{\Delta t}\begin{bmatrix} A^{p+1}_{mn} \\ B^{p+1}_{mn} \end{bmatrix} \tag{41}$$

where

$$\begin{aligned} D_{11} &= \alpha^2\delta_{nm} + \beta^2\delta_{nn} + \frac{1}{4\rho}(\delta_m \rho\alpha^2\delta_m + \delta_n\mu\delta_n) \\ D_{22} &= \alpha^2\delta_{nn} + \beta^2\delta_{mm} + \frac{1}{4\rho}(\delta_n \rho\alpha^2\delta_n + \delta_m\mu\delta_m) \\ D_{12} &= \left(\frac{\alpha^2-\beta^2}{4}\right)\delta_{mn} + \frac{1}{4\rho}(\delta_m\lambda\delta_n + \delta_n\mu\delta_m) \\ D_{21} &= \left(\frac{\alpha^2-\beta^2}{4}\right)\delta_{nm} + \frac{1}{4\rho}(\delta_n\lambda\delta_m + \delta_m\mu\delta_n). \end{aligned} \tag{42}$$

The Fourier transformation of the difference equations can be effected at this point by introducing the Fourier series

$$A^p_{mn} = \sum_{a,b} A^p_{ab}\ e^{i(ma + nb)\Delta x} \tag{43}$$

and similar expressions for B, R, and S with $\Delta x_1 = \Delta x_2 = \Delta x$. Under transformation the δ operators convert to multiplications by Sine functions of the wave numbers a and b and thus:

$$\begin{aligned} \delta_{mn} &= -4\ \mathrm{Sin}^2\left(\frac{a\Delta x}{2}\right) \\ \delta_{mn} &= -4\ \mathrm{Sin}(a\Delta x)\ \mathrm{Sin}(b\Delta x) \\ \delta_m &= +2i\ \mathrm{Sin}(a\Delta x)\ ,\ i = \sqrt{-1} \end{aligned} \tag{44}$$

$$D_{11} = -4\alpha^2 \mathrm{Sin}^2\left(\frac{a\Delta x}{2}\right) - 4\beta^2 \mathrm{Sin}^2\left(\frac{b\Delta x}{2}\right) + \frac{i}{2\rho}\left(\delta_m \rho\alpha^2 \mathrm{Sin}(a\Delta x) + \delta_n \mu \mathrm{Sin}(b\Delta x)\right)$$

$$D_{22} = -4\alpha^2 \mathrm{Sin}^2\left(\frac{b\Delta x}{2}\right) - 4\beta^2 \mathrm{Sin}^2\left(\frac{a\Delta x}{2}\right) + \frac{i}{2\rho}\left(\delta_n \rho\alpha^2 \mathrm{Sin}(b\Delta x) + \delta_m \mu \mathrm{Sin}(a\Delta x)\right)$$

$$D_{12} = -(\alpha^2-\beta^2)\mathrm{Sin}(a\Delta x)\mathrm{Sin}(b\Delta x) + \frac{i}{2\rho}\left(\delta_m \lambda \mathrm{Sin}(b\Delta x) + \delta_n \mu \mathrm{Sin}(a\Delta x)\right)$$

$$D_{21} = -(\alpha^2-\beta^2)\mathrm{Sin}(a\Delta x)\mathrm{Sin}(b\Delta x) + \frac{i}{2\rho}\left(\delta_n \lambda \mathrm{Sin}(a\Delta x) + \delta_m \mu \mathrm{Sin}(b\Delta x)\right.$$

The Fourier transformed matrix with summation over all wavelengths assumed takes the form

$$\begin{bmatrix} 0 & \frac{1}{\Delta t} I \\ \frac{1}{\Delta t} I & -I \end{bmatrix} \begin{bmatrix} A_{ab}^{p+1} \\ B_{ab}^{p+1} \\ R_{ab}^{p+1} \\ S_{ab}^{p+1} \end{bmatrix} = \begin{bmatrix} \frac{1}{\Delta x^2} \begin{bmatrix} D_{11} & D_{12} \\ D_{21} & D_{22} \end{bmatrix} & \frac{1}{\Delta t} I \\ \frac{1}{\Delta t} I & 0 \end{bmatrix} \begin{bmatrix} A_{ab}^{p} \\ B_{ab}^{p} \\ R_{ab}^{p} \\ S_{ab}^{p} \end{bmatrix} \qquad (45)$$

where I is a 2 x 2 identity matrix.

The amplification matrix can be found directly by computing the inverse of the matrix on the left and solving for the values at p + 1.

$$\begin{bmatrix} A_{ab}^{p+1} \\ B_{ab}^{p+1} \\ R_{ab}^{p+1} \\ S_{ab}^{p+1} \end{bmatrix} = \begin{bmatrix} \left(\frac{\Delta t}{\Delta x}\right)^2 D + I & \Delta t\, I \\ \frac{\Delta t}{\Delta x^2} D & I \end{bmatrix} \begin{bmatrix} A_{ab}^{p} \\ B_{ab}^{p} \\ R_{ab}^{p} \\ S_{ab}^{p} \end{bmatrix} = G \begin{bmatrix} A_{ab}^{p} \\ B_{ab}^{p} \\ R_{ab}^{p} \\ S_{ab}^{p} \end{bmatrix} \qquad (46)$$

The problem of stability for the P-SV equations of motion is thus reduced to that of finding the estimates for the bounds of powers of the amplifications matrix G. The Von Neumann (Necessary) Condition for stability requires that the maximum eigenvalue (ζ) be less than or equal to one. The equation for the eigenvalue which is derived from the determinant of G is thus:

$$(1 - (2 + D_{11})\zeta + \zeta^2)(1 - (2 + D_{22})\zeta + \zeta^2) - D_{12}D_{21}\zeta^2 = 0 \tag{47}$$

which can be written

$$(\zeta^2 - 2A_1\zeta + 1)(\zeta^2 - 2A_2\zeta + 1) \tag{48}$$

Thus,
$$\zeta = A_1 \pm \sqrt{A_1^2 - 1} \tag{49}$$

and
$$\zeta = A_2 \pm \sqrt{A_2^2 - 1}$$

where

$$A_1 = \frac{1}{2}\left[2 + \frac{1}{2}(D_{11} + D_{22}) + \sqrt{\left(\frac{D_{11}-D_{22}}{2}\right)^2 + D_{12}D_{21}} \right]$$

$$A_2 = \frac{1}{2}\left[2 + \frac{1}{2}(D_{11} + D_{22}) - \sqrt{\left(\frac{D_{11}-D_{22}}{2}\right)^2 + D_{12}D_{21}} \right]$$

For stability by the Von Neumann condition $|\zeta| < 1 + 0(n\Delta t)$ where $0(n\Delta t)$ is the maximum allowable error at the end of computation. However, the solutions for ζ with a gradient involve complex numbers and all the eigenvalues can not be less than or equal to one. This is a consequence of the change in amplitude inherent in the propagation of seismic waves into different velocity media. The eigenvalues determine the change in amplitude in propagation across an interface. The product of the eigenvalues, however, is unity indicating that on propagating back across the interface in the opposite direction the

amplitudes are stable. The stability of the finite difference equations and velocities used in this study have been checked numerically for typical and extreme values by computing $|\zeta|$ for selected wave numbers.

For homogeneous media the conditions for stability can be computed directly by using only the real parts of the amplification matrix in the expression for A and noting that the inequality $|A| < 1$ can be written as $0 < (1-A)/2 < 1$,

$$0 < \left(\frac{\alpha^2+\beta^2}{\alpha^2}\right)\left[\mathrm{Sin}^2\left(\frac{a\Delta x}{2}\right) + \mathrm{Sin}^2\left(\frac{b\Delta x}{2}\right)\right]$$

$$\pm \left(\frac{\alpha^2-\beta^2}{\alpha^2}\right)\sqrt{\left(\mathrm{Sin}^2\left(\frac{a\Delta x}{2}\right) - \mathrm{Sin}^2\left(\frac{b\Delta x}{2}\right)\right)^2 + \frac{1}{4}\,\mathrm{Sin}^2(a\Delta x)\mathrm{Sin}^2(b\Delta x)} \qquad (50)$$

$$< 2 \,/\, \alpha^2\left(\frac{\Delta t}{\Delta x}\right)^2$$

All quantities are positive and the radical is always less than the first term. The most severe conditions occur where $a\Delta x = b\Delta x = \pi$ and gives (Alterman and Loewenthal, 1970)

$$\alpha < 1/\left(\frac{\Delta t}{\Delta x}\right)\sqrt{1+\left(\frac{\beta}{\alpha}\right)^2}\,. \qquad (51)$$

Typical values used in this study imply stability up to a P-wave velocity of 8.66 in the homogeneous portion of the grid. The highest velocity used was 7.0.

Results

Introduction The variety of velocity structures in which seismic waves can be propagated theoretically by a finite difference scheme for a general inhomogeneous media is endless. The only real limiting factors are the size of the computation grid required to give the desired accuracy and the time required to carry out the computations in the computer. Consequently this study has been restricted to the general computation scheme shown in Figure 3. A line source was assumed at the origin. Finite difference computations were carried out in the depth range of five to nine kilometers. The velocity above five kilometers was four km/sec. Structures in the velocity were placed in the depth range of six to eight kilometers. These included various examples of velocity gradients, boundaries, and upward or downward displaced faults. The velocity below eight and a half kilometers was assumed constant (usually six km/sec). Shear wave velocities were generally computed from the compressional wave velocities by assuming Poisson's ratio. For display purposes the data were saved at selected points in the media and used to generate theoretical seismograms. Also, the theoretical displacements were printed at selected times or converted to dilatation and rotation and printed for direct observation of the wave motion. The conversion to rotation allowed direct observation of the shear phases which otherwise would have been lost in the higher amplitude compressional phases. Although the depths and velocities assumed here are appropriate for a deep sedimentary basin, the velocities and distances can be scaled to fit other cases of interest in seismology.

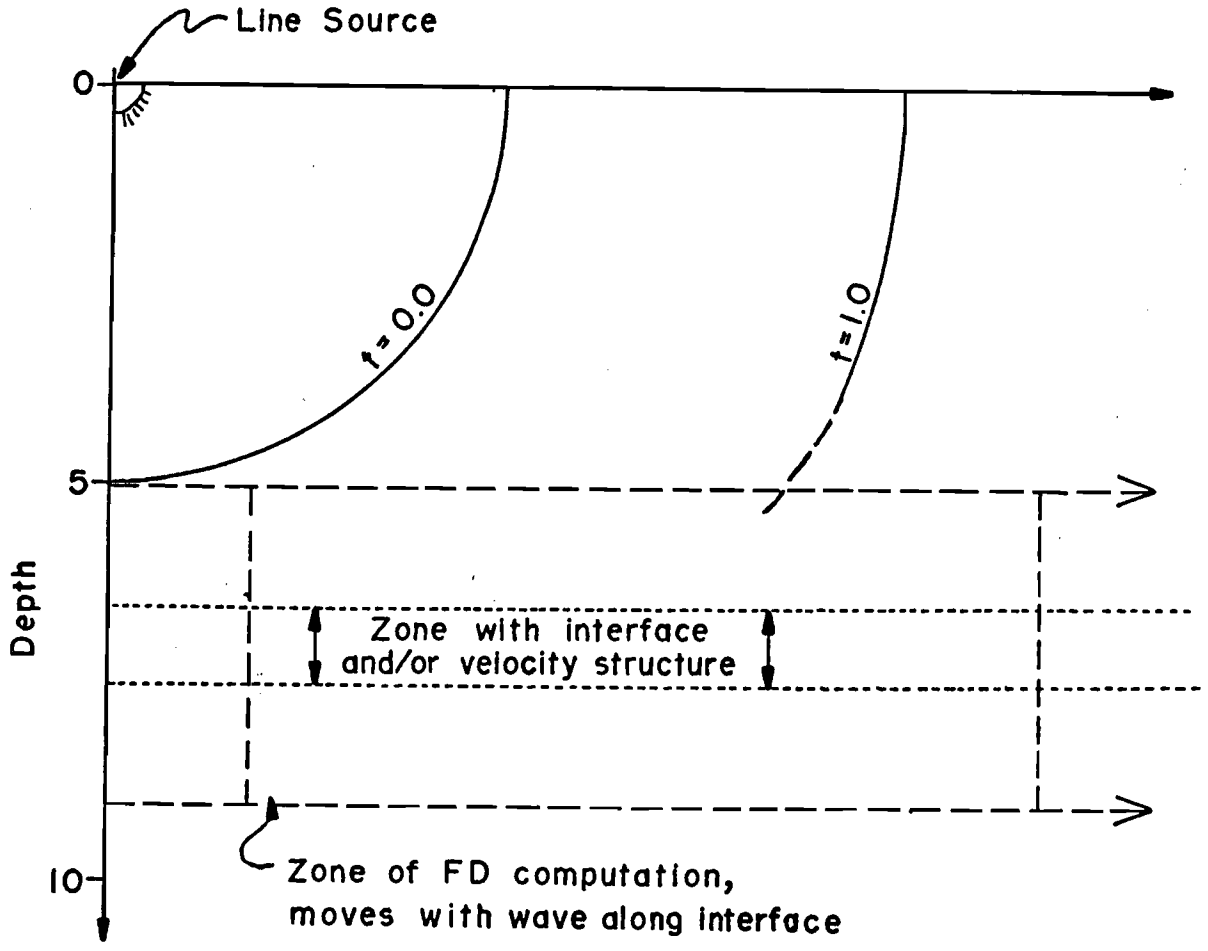

Figure 3. Geometry of general computation scheme used in finite difference calculations.

A sharp gradient was examined first to investigate deviations from the theoretically predicted results for a welded contact between two homogeneous media. The gradient extended over two grid units. For the source used this was equivalent to about 0.2 wavelengths. The finite difference case for the welded contact involves an implicit equation and was not computed. Examples of various gradients were then computed to examine the effects of the gradients on the amplitudes of the head and reflected waves. Finally, upward and downward faults were computed to examine their effect on the generation of head and reflected waves.

The Sharp Velocity Gradient A sharp velocity gradient extending over only two grid invervals is the closest approximation to a welded contact possible without solving an implicit equation for each time step in the finite difference formulism. For computation the interface was placed near the center of the grid. The finite difference computation was initiated when the cylindrical pulse was incident on the top of the grid. With computer printouts of the grid at 0.25 second invervals to six seconds covering the propagation of the waves along the boundary to a distance of 33 kilometers, it was necessary to choose zones which best illustrated the formation or character of the waves interacting with the boundary. Figure 4 illustrates the wave fronts for the refracted and head waves generated with the velocities used in this study. A number of regions in the wavefronts are of particular interest because of the difficulty in obtaining solutions through other mathematical methods. These include (1) the amplitudes of the reflected and head waves near the critical angle, (2) the leading edge of the head waves and (3) the

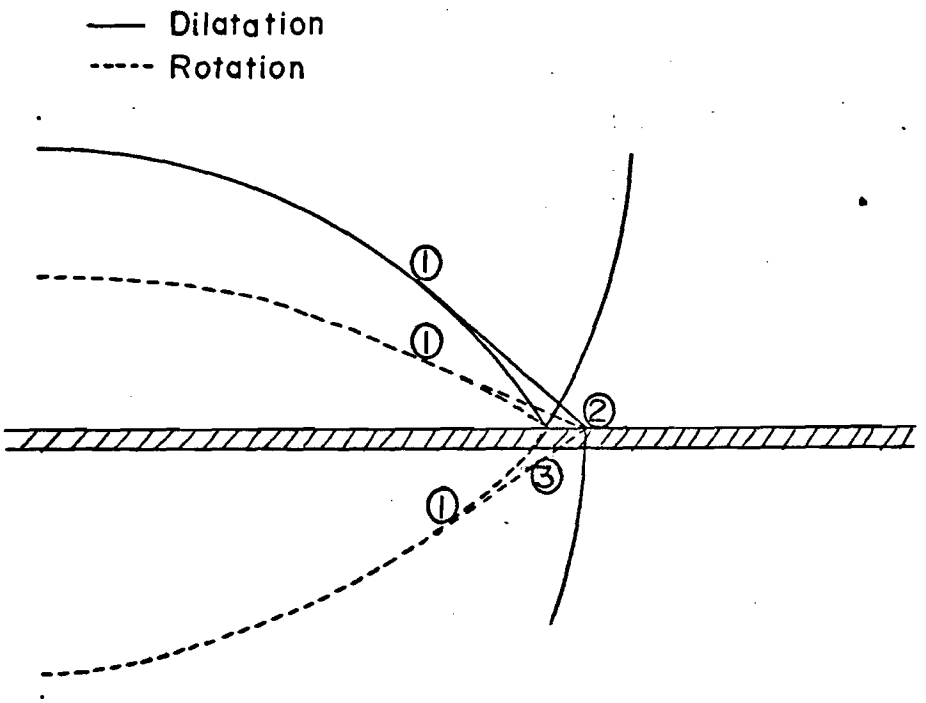

Figure 4. Wave fronts of reflected and refracted waves generated by an incident compressional wave.

displacement in the lower media caused by the direct wave beyond the critical angle.

The compressional and shear reflected waves occur without interference at angles less than critical and their amplitudes can be measured directly. The amplitudes are best observed at angles of incidence of 20 to 30 degrees. For comparison the Zopritz equations have been solved for the theoretical amplitudes of the reflected and refracted phases expected for the velocities used in the sharp gradient (Figure 5). Figures 6a and 6b show the finite difference reflected dilatation and shear waves. The line-printer output has been contoured in the region of the maximum amplitude of the reflected phases to emphasize the amplitude variations. Selected interpreted amplitudes from the finite difference printout are shown in Figure 7 and compared to the theoretical ratio of incident to reflected wave amplitudes. The amplitudes are corrected for cylindrical spreading. The compressional waves are about 10 percent larger than the theoretical and the amplitude minimum may be shifted to higher angles of incidence. The amplitude variation and shift may be partially accounted for by the effect of the sharp gradient layer at the boundary. The reflected shear wave amplitudes also show a shift or are perhaps a few percent less than expected at 20 to 30 degrees angle of incidence.

A more precise measure of the amplitudes of the compressional reflections can be obtained from the finite difference seismograms of the dilatation (Figure 8a-d). The receiver at 5.0 kilometers (32^{o} angle of incidence) indicates an amplitude ratio of 0.18 ± 0.01, which falls on the theoretical curve. However, the value at 3.5 kilometers (24^{o} angle of incidence) indicates an amplitude ratio of

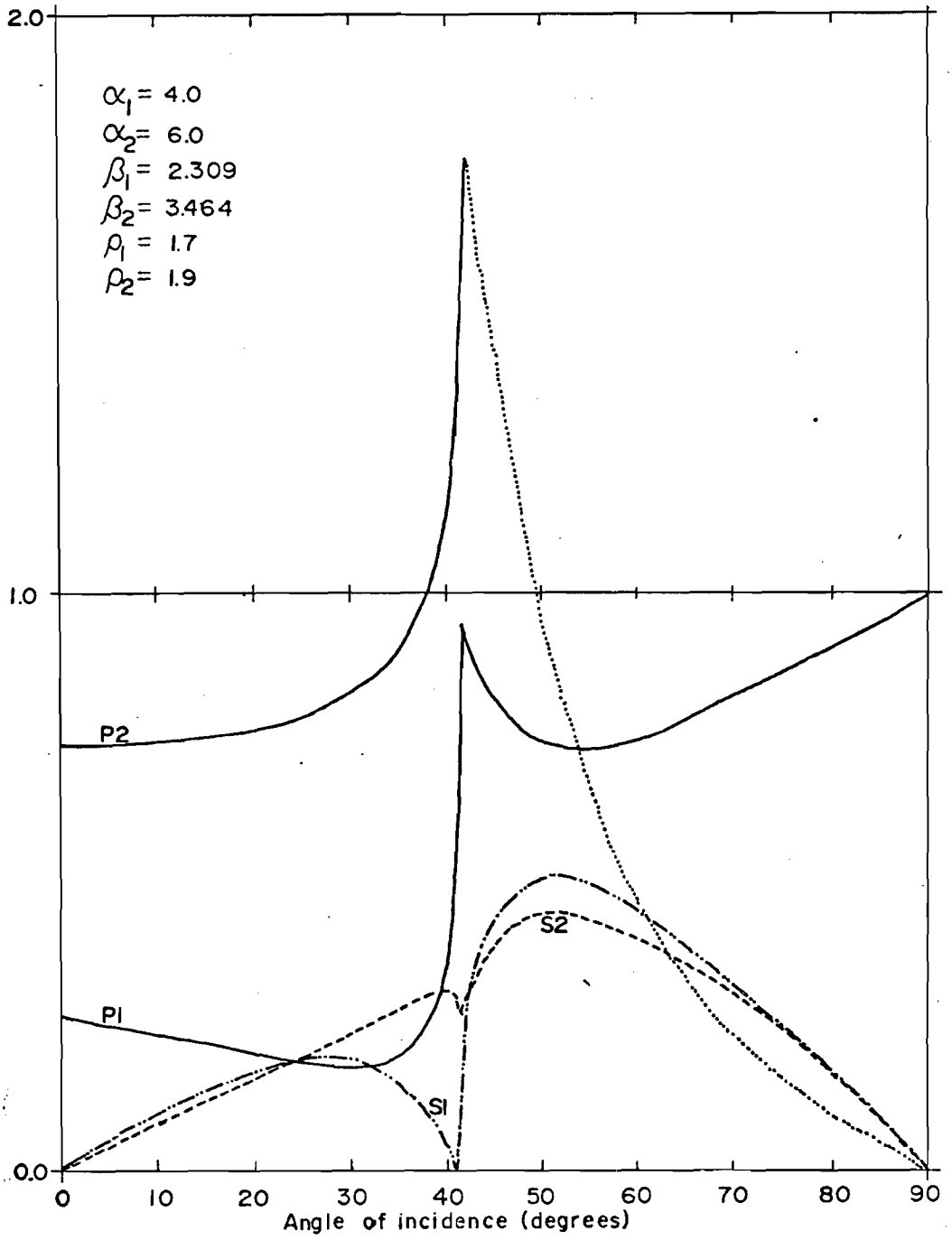

Figure 5. Solution of Zopritz equations for the ratio of incident amplitude for an incident compressional wave to reflected ampliutde.

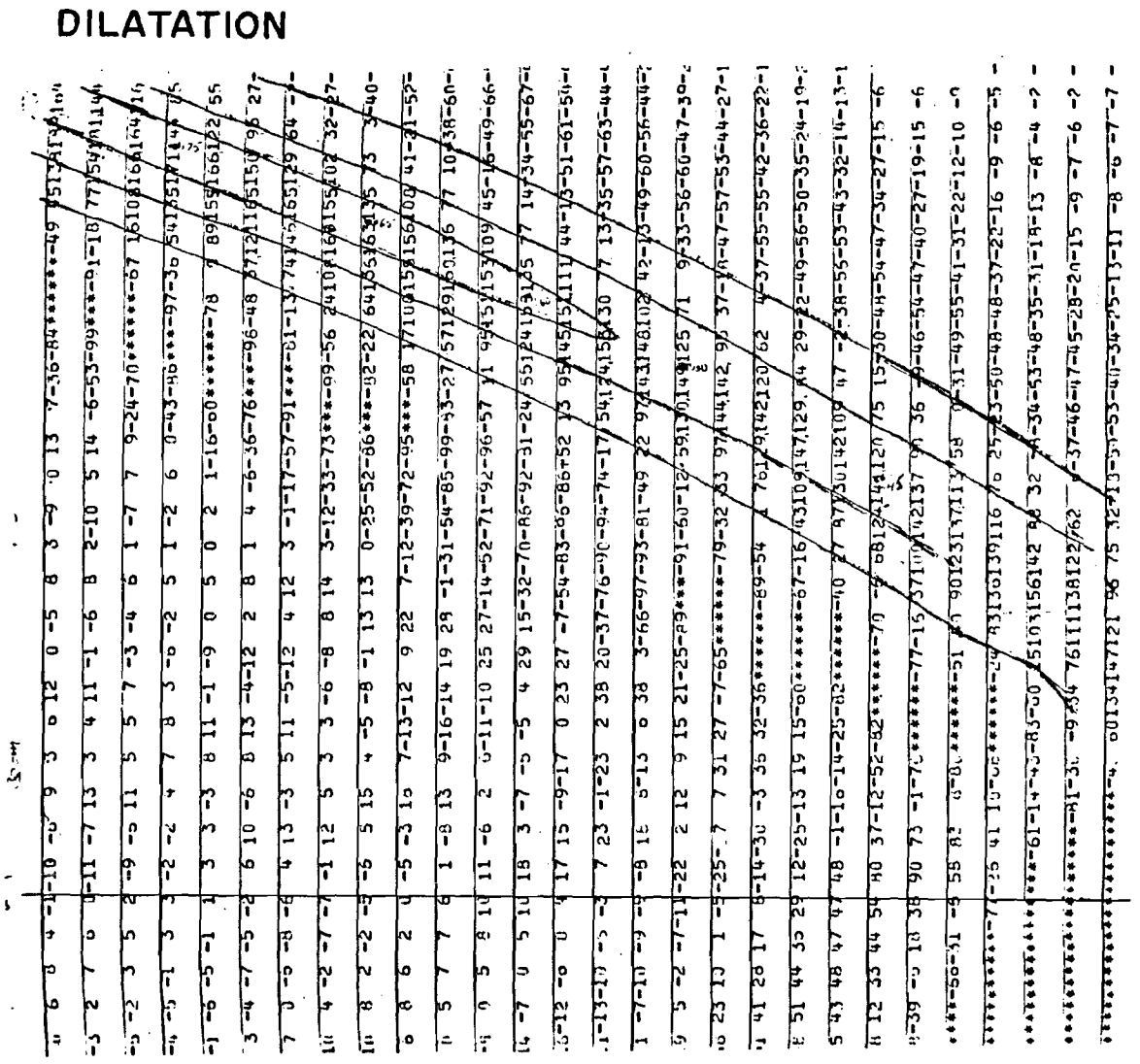

Figure 6a. Finite difference grid of dilatation showing amplitudes of compressional wave reflections.

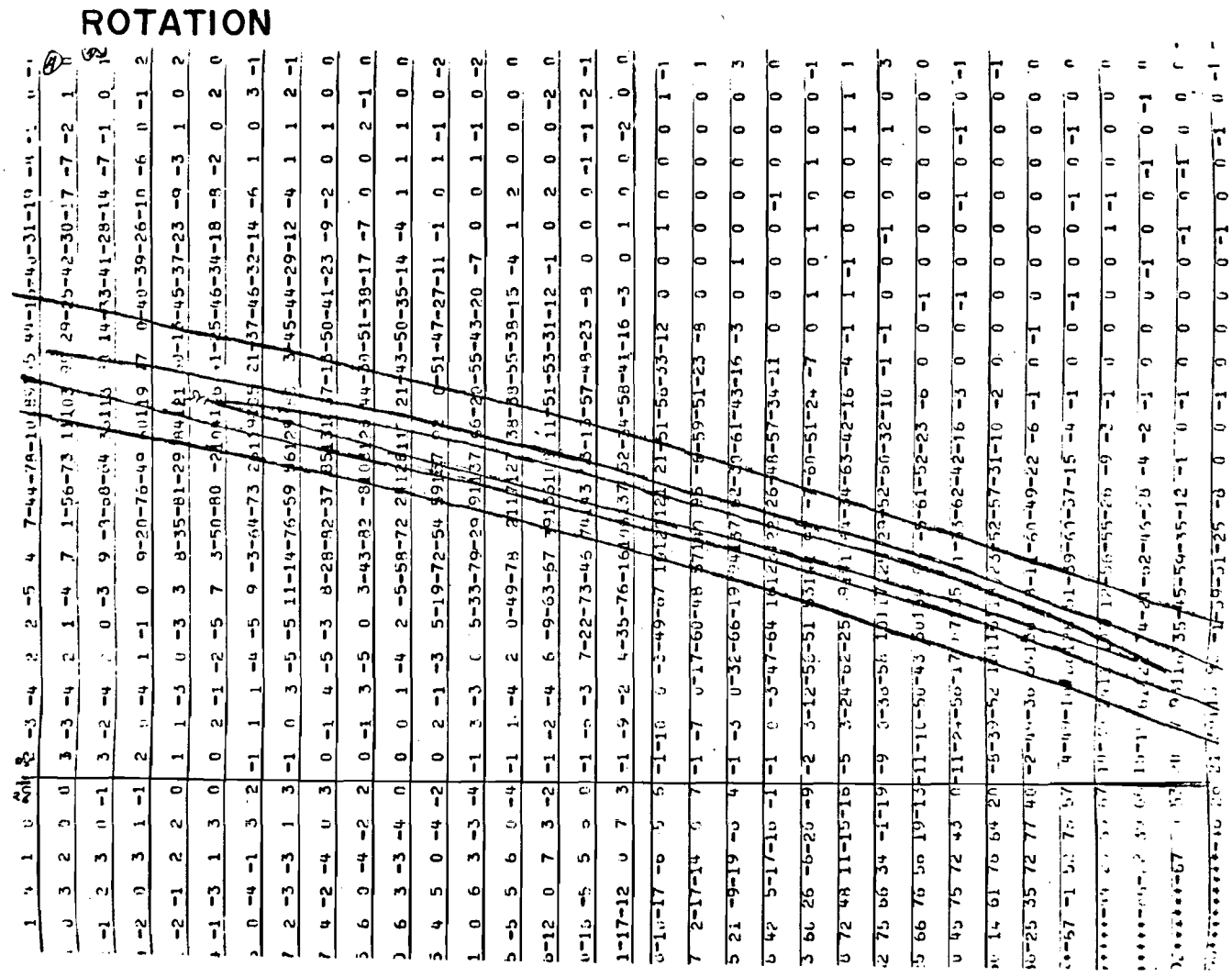

Figure 6b. Finite difference grid of rotation showing amplitudes of shear wave reflection.

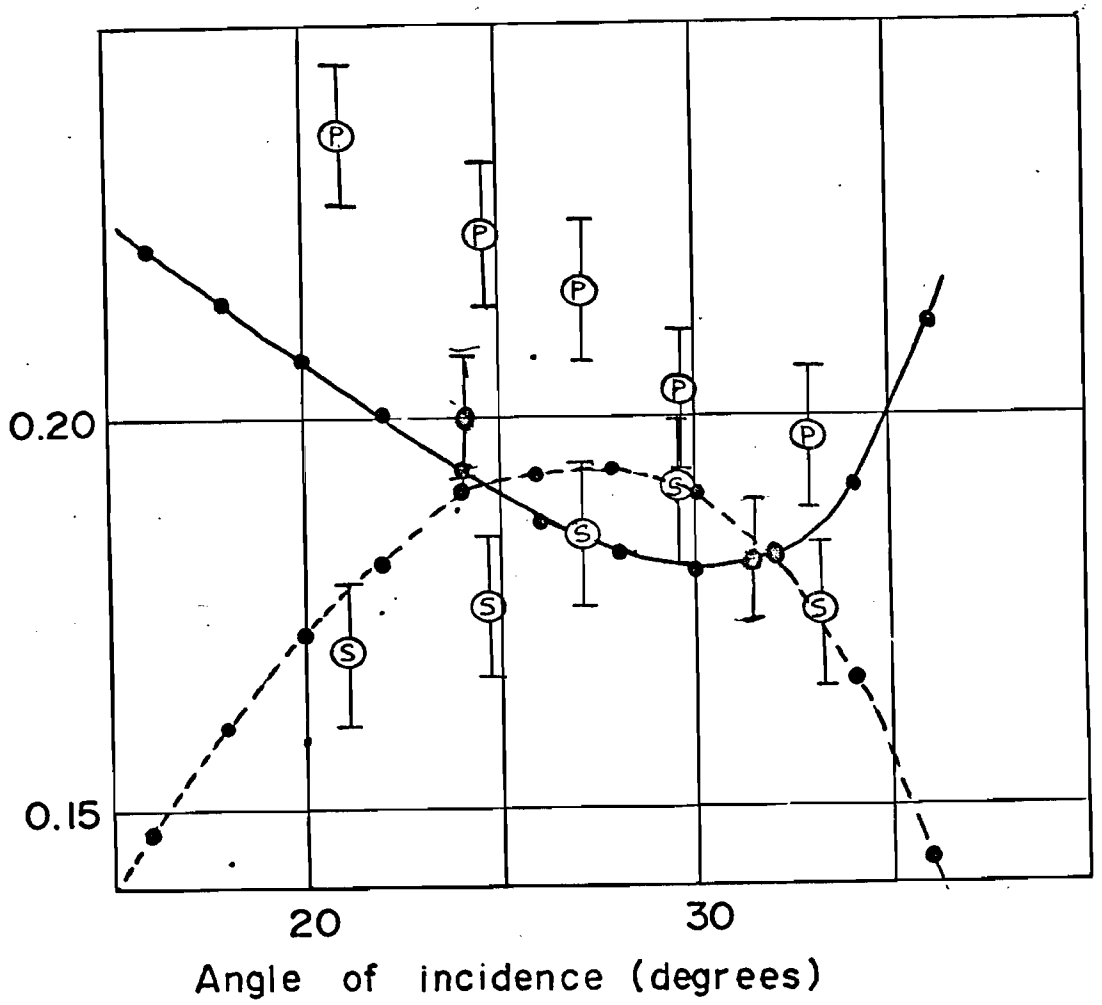

Figure 7. Comparison of observed finite difference amplitudes with theoretical reflection coefficients.

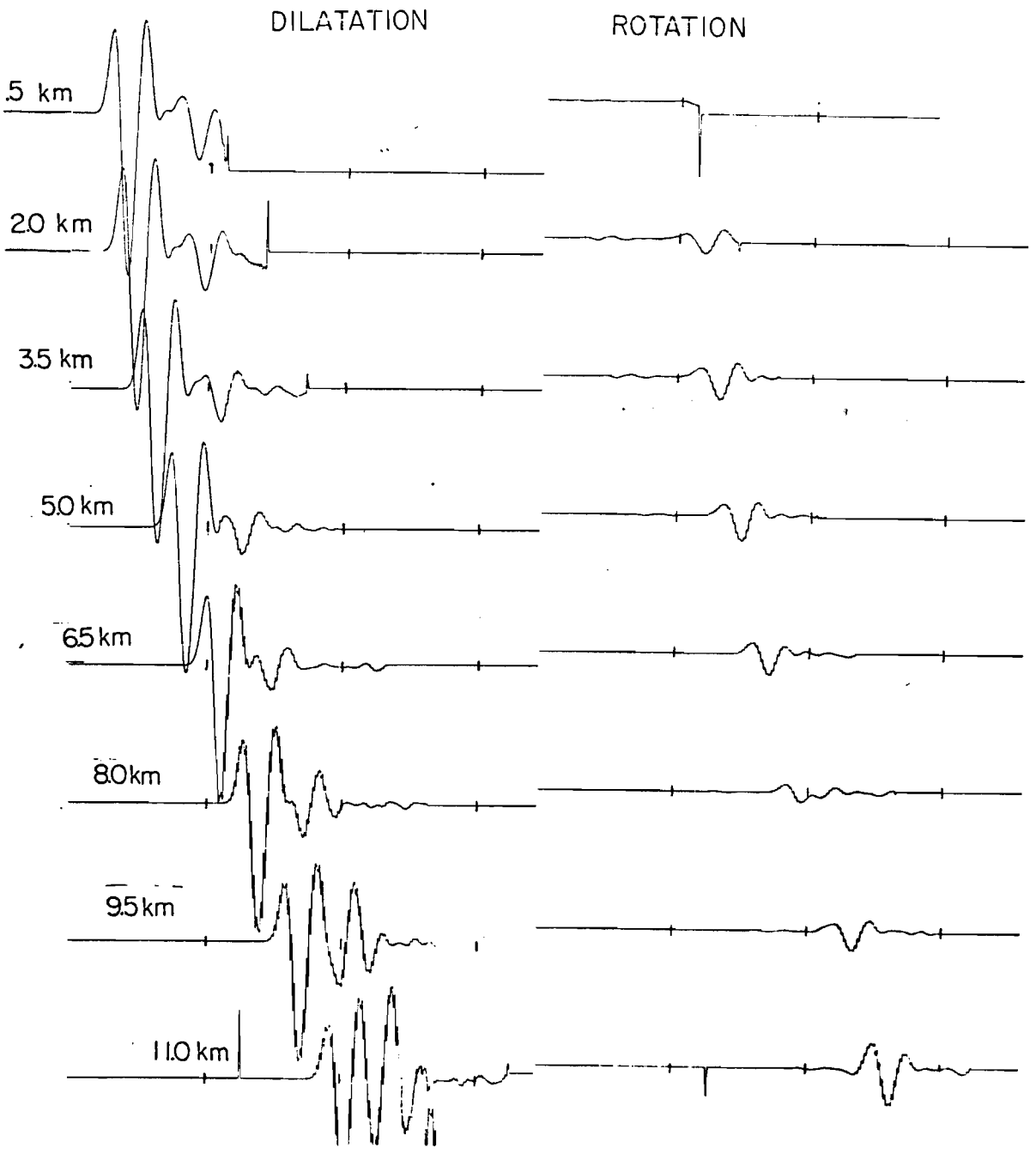

Figure 8a. Theoretical seismograms showing dilatation and rotation from 0.5 to 11.0 kilometers for a sharp gradient with "seismometer" placed one kilometer above interface.

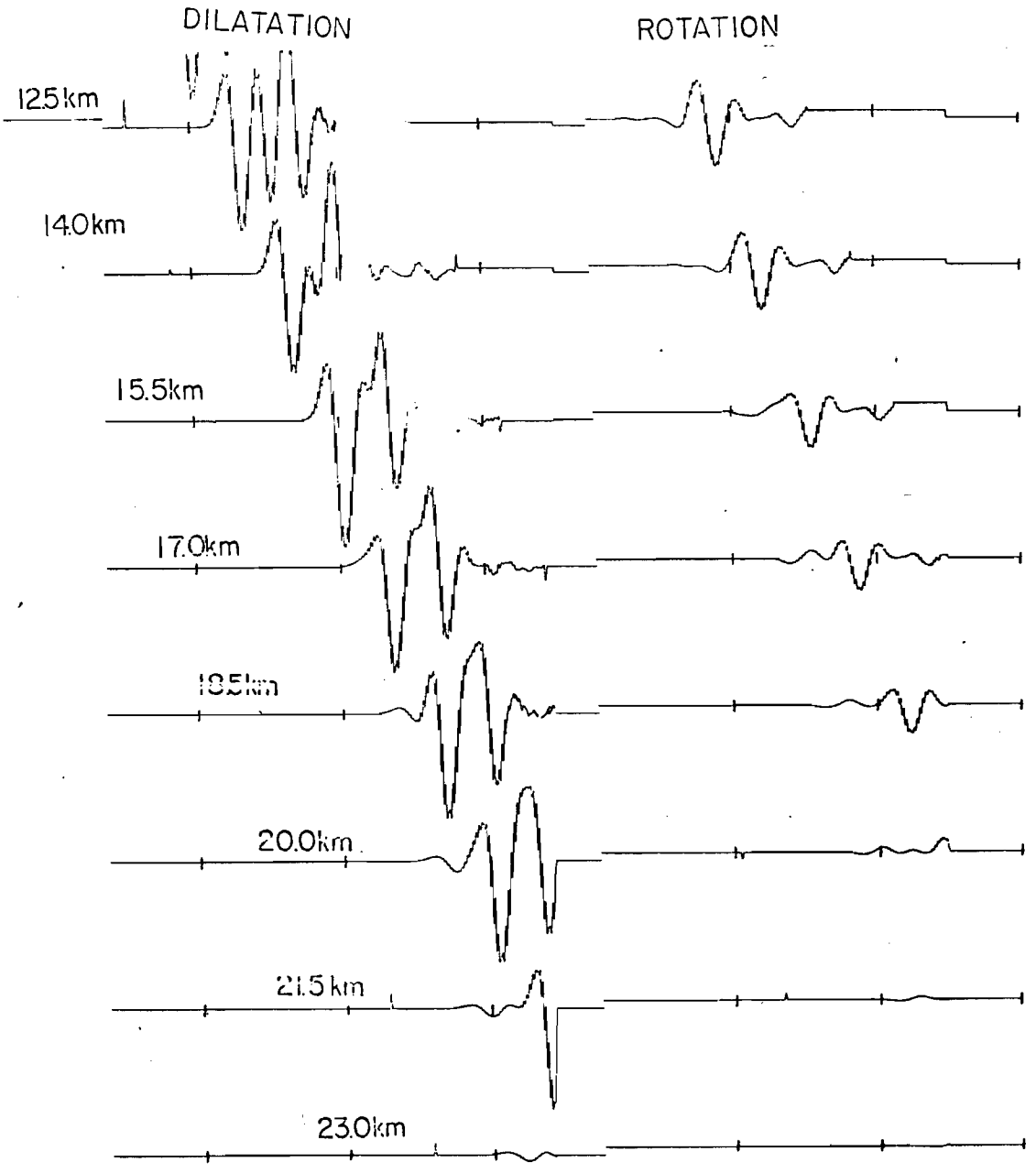

Figure 8b. Theoretical seismograms showing dilatation and rotation from 12.5 to 23.0 kilometers for a sharp gradient with "seismometer" placed one kilometer above interface.

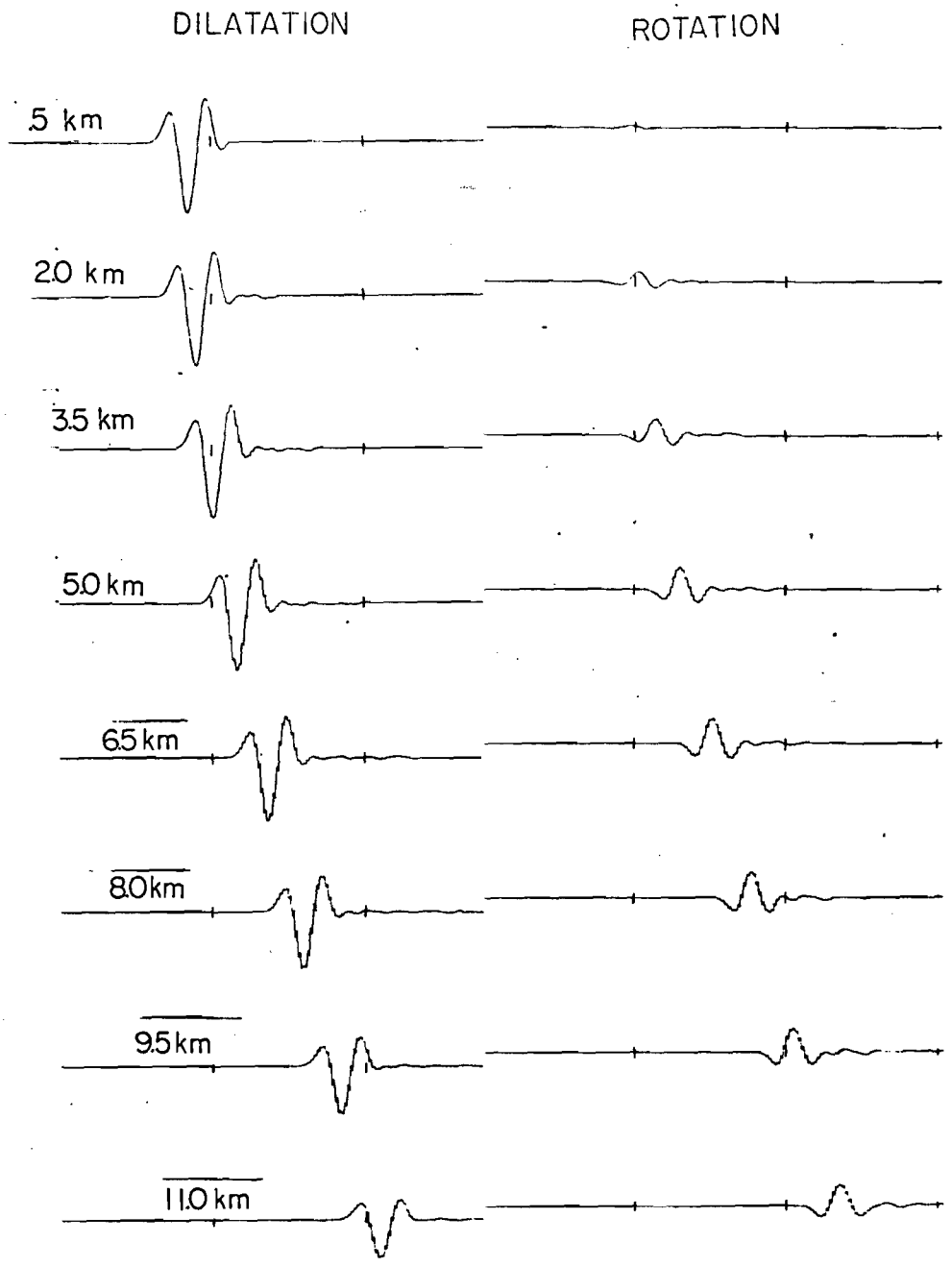

Figure 8c. Theoretical seismograms showing dilatation and rotation from 0.5 to 11.0 kilometers for a sharp gradient with"seismometer" placed one kilometer below interface.

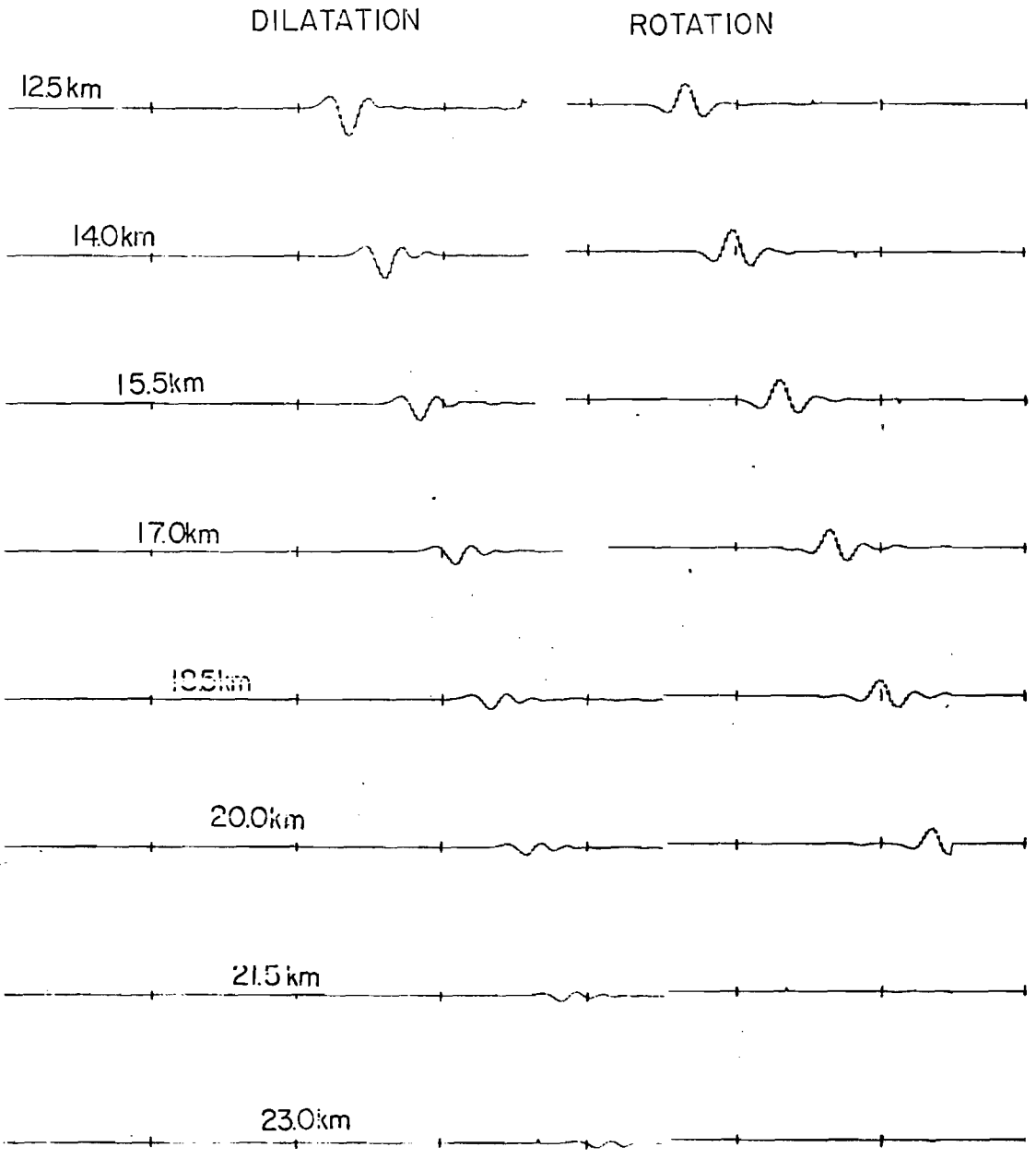

Figure 8d. Theoretical seismograms showing dilatation and rotation from 12.5 to 23.0 kilometers for a sharp gradient with "seismometer" placed one kilometer below interface.

0.20 ± 0.01 which is higher than the expected curve supporting the interpreted amplitudes from the finite difference printout. In Figure 8 the increased amplitudes of the reflected phases beyond the cricital angle are easily observed but direct measurement is difficult because of interference with the direct arrival. The reflected shear wave amplitudes go through the expected minimum near 8.0 km. In Figure 8c and 8d the character of the direct wave in the lower media can be seen to be continuous and similar to that of the incident pulse. However, the effect in the lower media of the reflected compressional wave beyond the critical angle causes an apparent continued oscillation of the refracted wave at distances beyond fourteen kilometers.

All three possible head waves are apparent in Figure 8. The character of the compressional head wave at 21.5 or 23 kilometers in the upper media is indistinguishable from the direct arrival which is observable at 0.5 kilometers. To be of the character of the potential only one cycle of motion should be apparent and the period should be longer. However, the period is the same as the direct arrival and the wavelet contains three half-cycles. The shear head wave in the upper media also shows the character of the direct arrival but is of opposite sign. The shear head wave in the lower media is the weakest phase observed. Its character is also similar to the character of the direct arrival. The head waves observed using the finite difference method have the character of the source pulse, not its potential.

The character of the reflected and head waves near the critical angle can be seen in Figure 9a and 9b. Where the critical distance

125 TIME STEPS

DILATATION

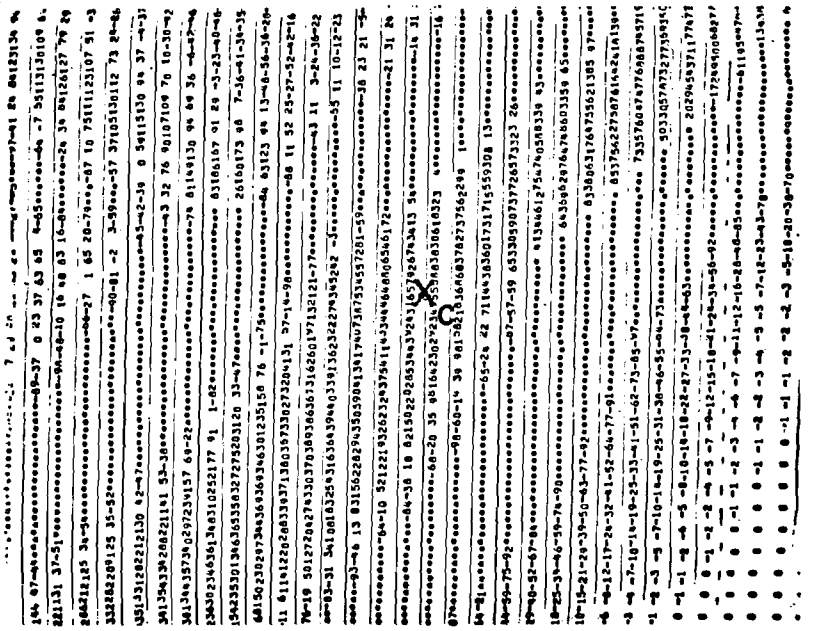

ROTATION

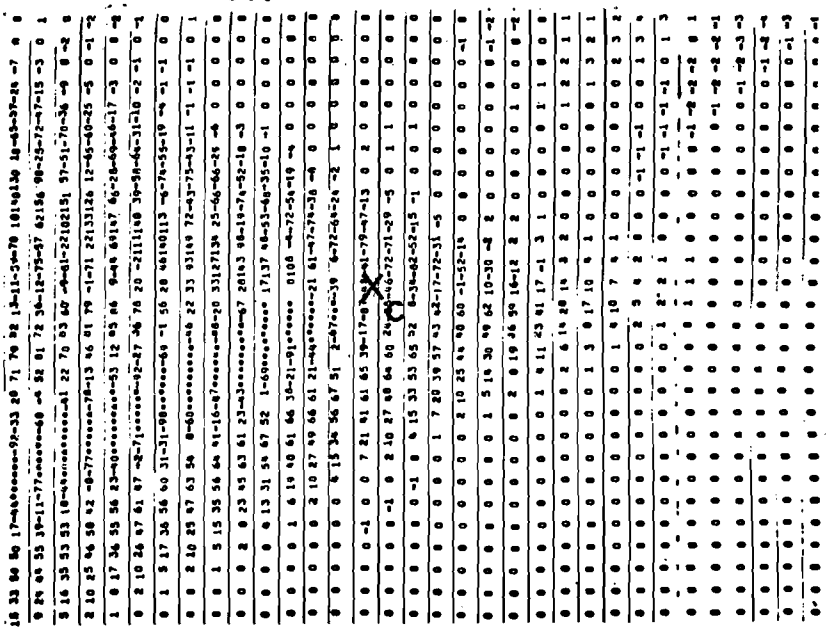

Figure 9a. Dilatation and Rotation grid values near the intersection of the critical angle of reflection with the interface.

175 TIME STEPS

DILATATION

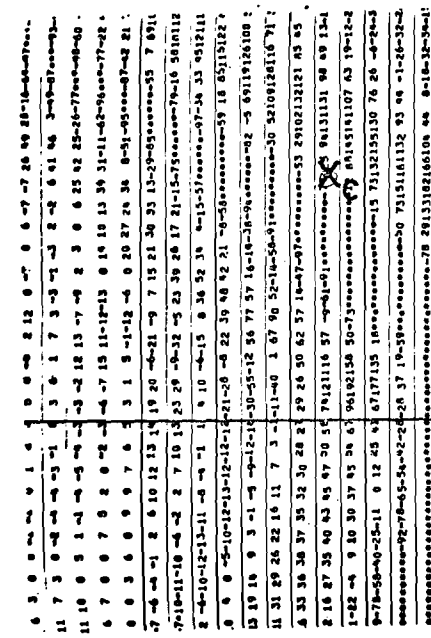

ROTATION

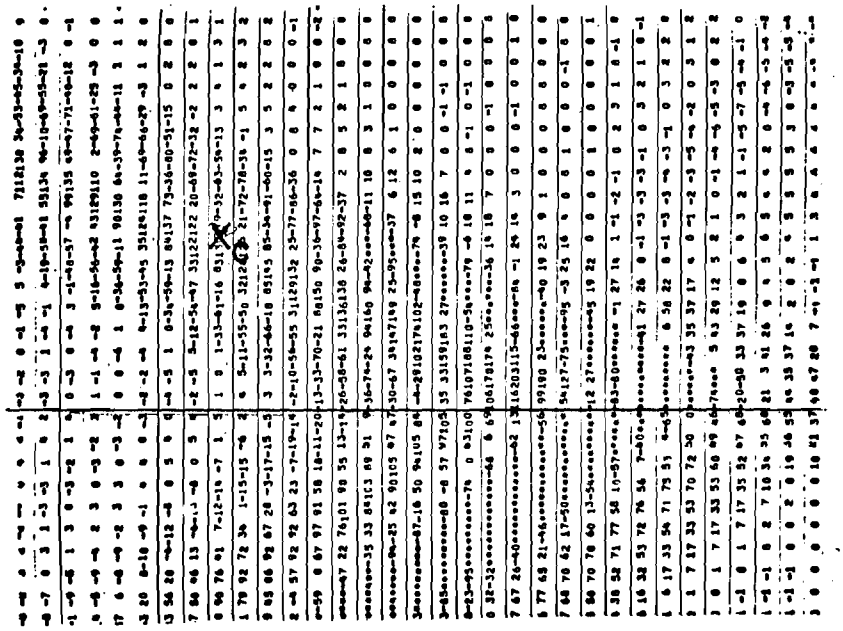

Figure 9b. Dilatation and rotation grid values near the intersection of the critical angle of reflection with isolated reflected wave above the interface.

corresponds to the intersection of the direct wave with the interface (Figure 9a), the dilatation is dominated by a continuous direct and refracted wave. At the critical angle in the reflected wave (Figure 9b) the strong increase in amplitude attributable to total reflection is apparent. The nature of the junction of the head wave and reflection is easiest to see in the rotation. The amplitudes are continuous and the head wave joins the reflected wave smoothly. The shear head waves emerge from the reflected or refracted phases smoothly and are virtually inseparable where they interfere.

Figure 10 shows the character of the dilatation and rotation at a point where the head wave has separated from the direct or reflected phases. The amplitudes are not constant across the boundary but show the effect of the transfer of energy from the direct refracted wave into the head wave. Figure 11 shows the penetration into the lower media of the reflected and incident pulse beyond the cricical angle. By comparison of the amplitudes in the lower media the penetration is seen to decrease with increased angle of incidence. However, some interference in the character of the wave motion is related to the generation of the refracted shear wave. Also, at 300 time steps in Figure 11 the head wave may cause some interference.

Effect of Velocity Gradients Figure 12 shows the waves recorded at the same relative position with a positive and negative gradient in the lower media. The gradient is 0.5 kilometers thick and the velocity at the boundary is 5.5 and 6.5 km/sec for the positive and negative gradient respectively. As in the sharp-gradient data presented previously the velocities are 4.0 and 6.0 kilometer/sec in the upper and lower media. The most obvious differences in the arrivals can be explained by the travel time variations expected. The

400 TIME STEPS

DILATATION

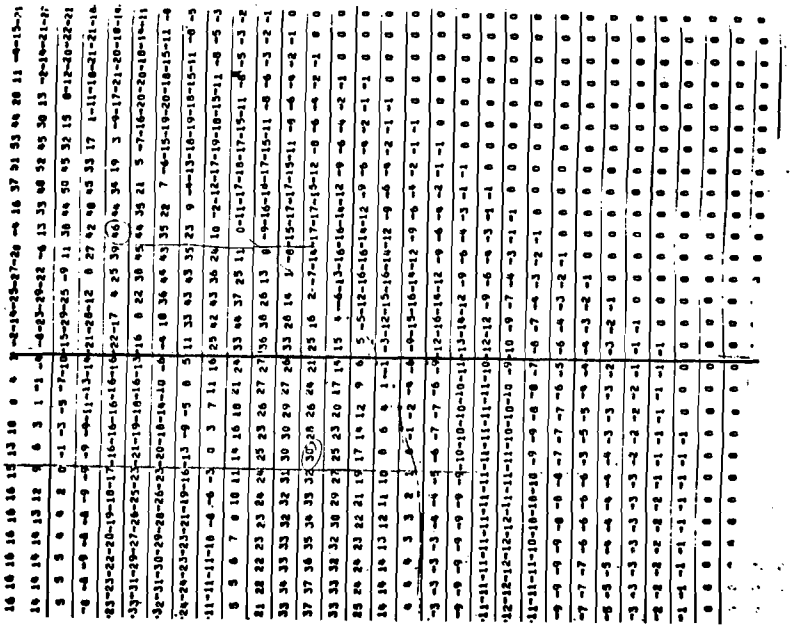

ROTATION

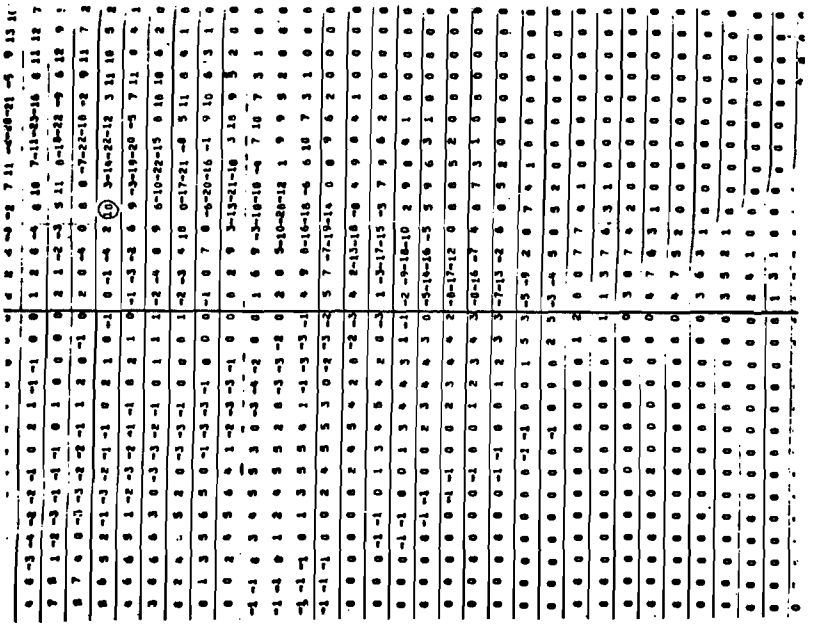

Figure 10. Dilatation and rotation components of the isolated head wave at the interface.

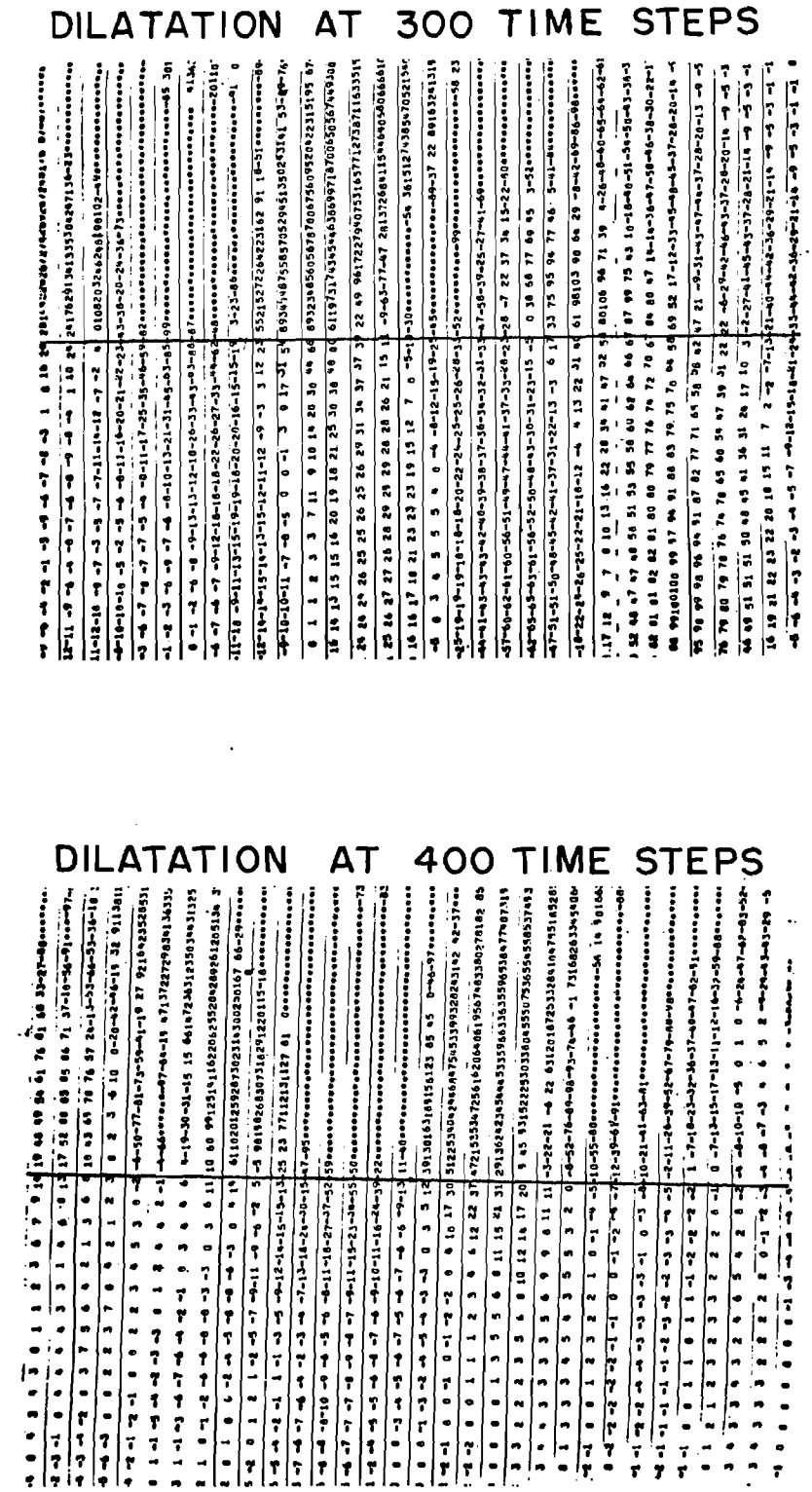

Figure 11. Penetration into the lower media of compressional waves beyond the critical angle.

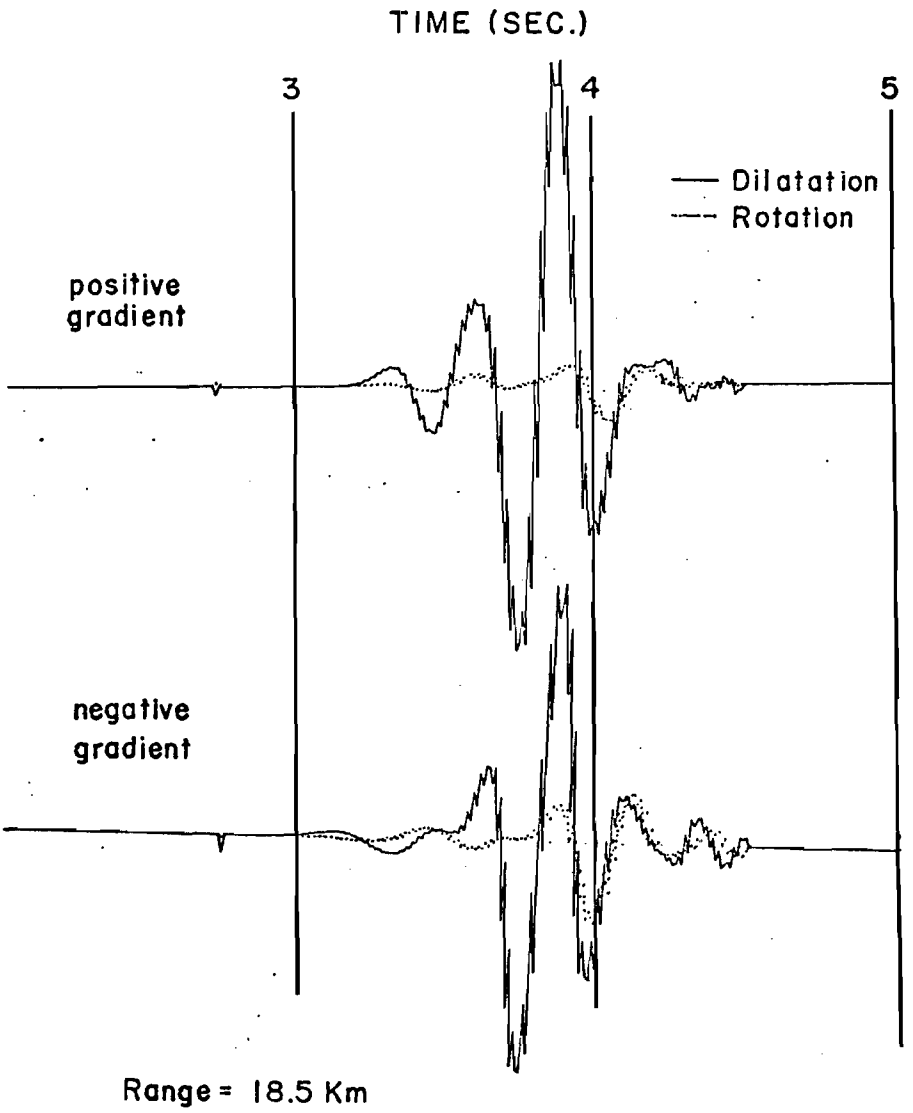

Figure 12. Theoretical seismograms showing the effects of gradients in the lower media.

effect of the positive gradient is to apparently increase the amplitudes of the head wave and decrease the reflected shear wave. The negative gradient decreased the compressional head wave and increased the reflected shear waves. A significant effect on the shear head wave was not observed.

Figure 13 shows the effect of a positive gradient 0.5 kilometers thick above the boundary from a velocity of 4.0 km/sec to 4.5 km/sec. Figures 13a, 13b and 13c represent a positive, zero and negative gradient, respectfully, below the boundary. The gradients are the same as were used in Figure 12. Apart from the obvious differences related to the expected variations in travel times, the compressional head waves show slightly increased amplitudes with the positive gradients. The reflected compressional waves are larger with a positive gradient. The greatest difference occurs in the reflected shear phases. At low angles of incidence the negative and positive gradient increase the shear phases beyond the critical angle. The distribution of dilatation and rotation for the arrivals of Figure 13a are shown in Figure 14a at 3.50 seconds and Figure 14b at 4.25 seconds. The contours of Figure 14 show that the gradient causes a decrease in amplitudes near the boundary. This perhaps accounts for an initial increase in the amplitudes in the head wave. The gradient also has a strong effect on the depth of penetration into the lower media. The waves at greater angles of incidence do not penetrate as deep.

Effect of a Fault Examples of finite difference head wave propagation are used here to illustrate the effect of a fault. The fault is at 16 kilometers which is just beyond the point where the head wave beings to separate from the reflected phase. The vertical

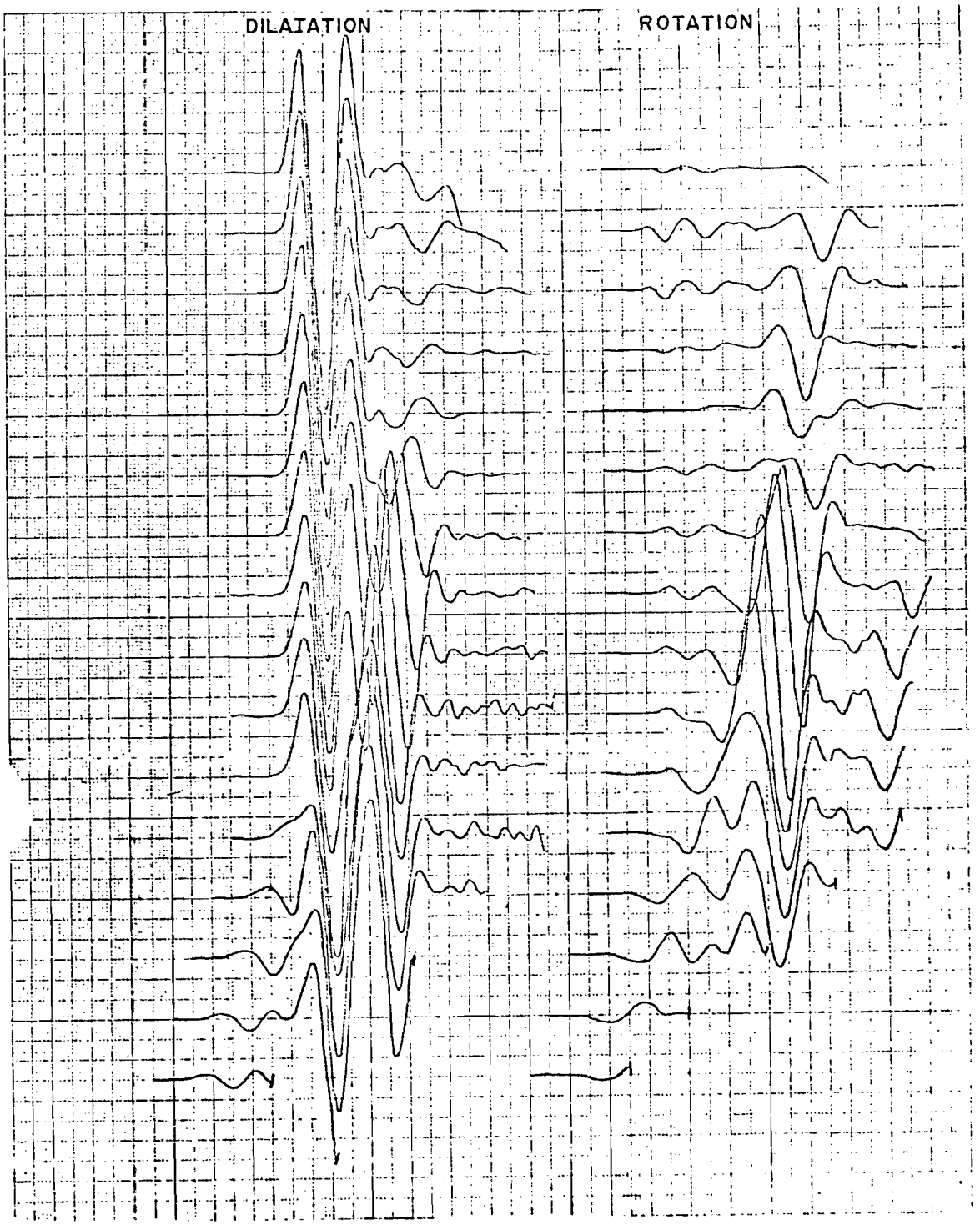

Figure 13a. Theoretical seismograms of the dilatation and rotation near a boundary with a positive gradient above and a positive gradient below.

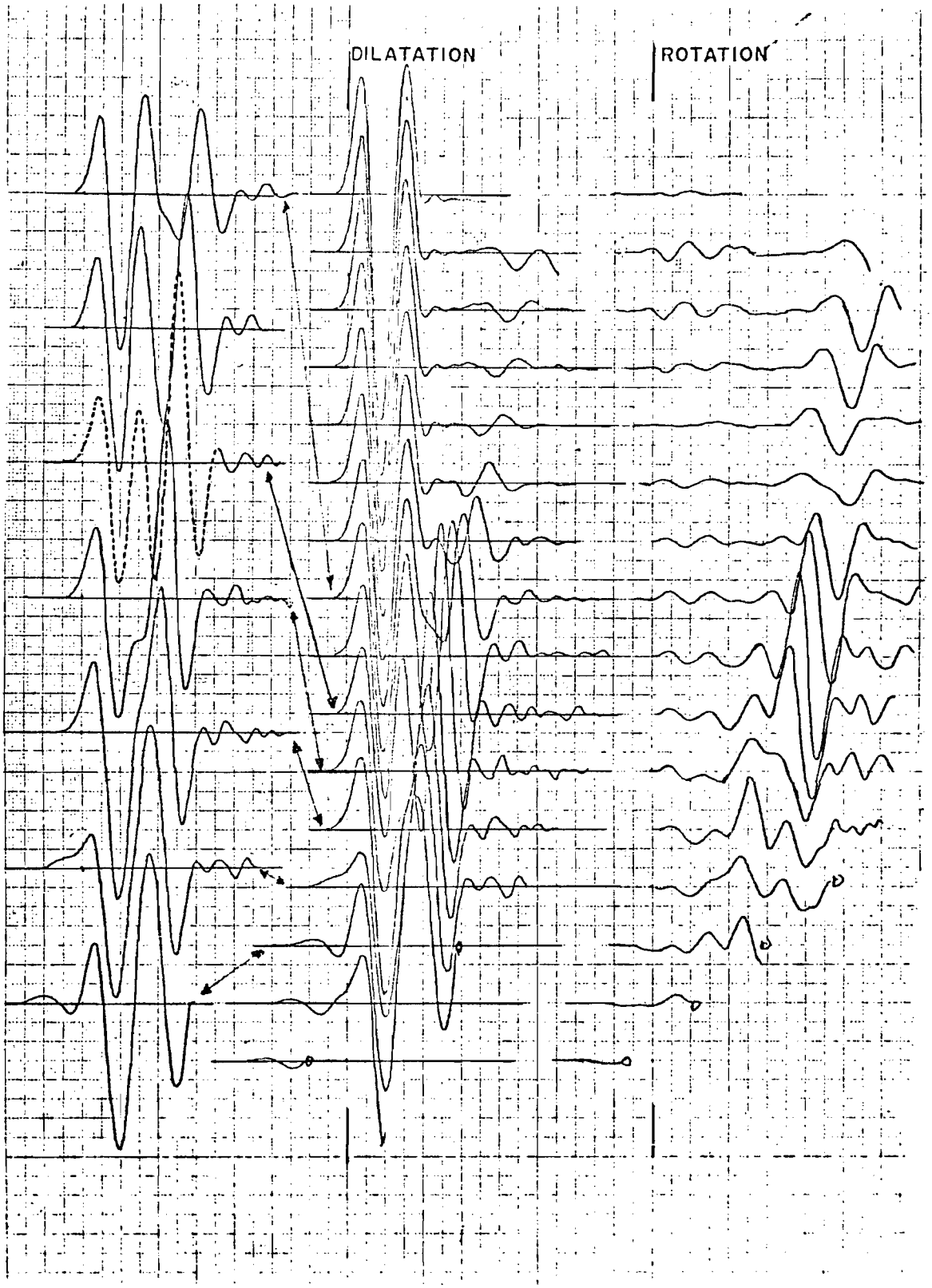

Figure 13b. Theoretical seismograms of the dilatation and rotation near a boundary with a positive gradient above and no gradient below.

Figure 13c. Theoretical seismograms of the dilatation and rotation near a boundary with a positive gradient above and a negative gradient below.

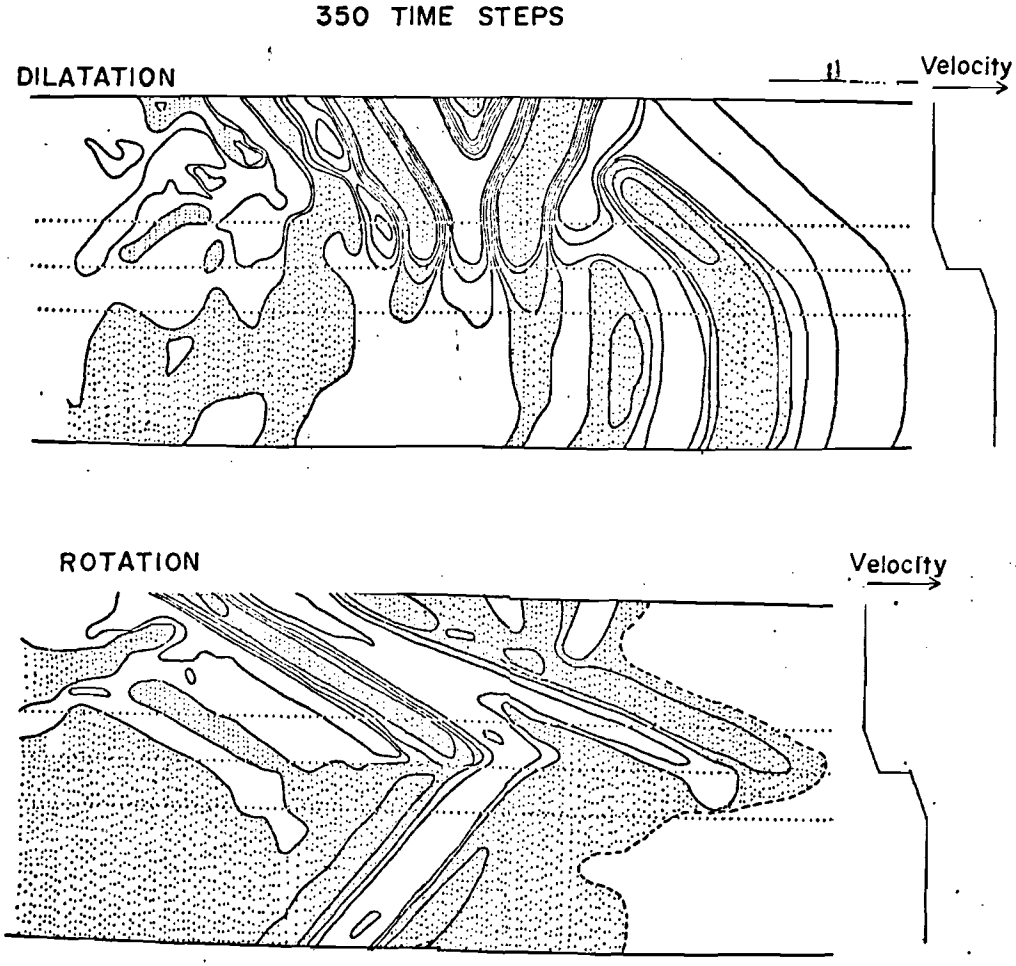

Figure 14a. Contoured grid values of dilatation and rotation at 3.50 seconds.

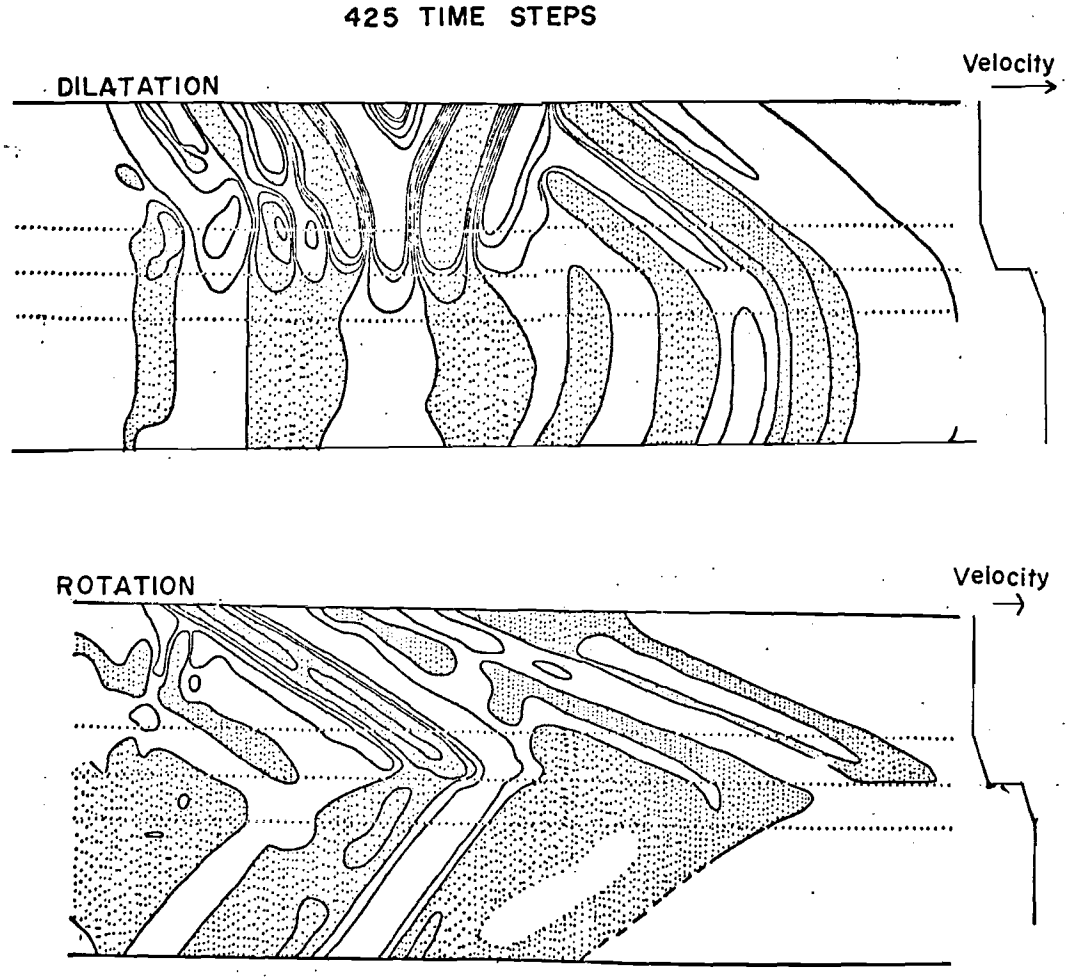

Figure 14b. Contoured grid values of dilatation and rotation at 4.25 seconds.

particle displacements at 1.5 kilometer intervals, 1.0 kilometers above the interface, are shown in Figure 15 for a 0.4 kilometer downward fault. The delay is evident in Figure 15 where the theoretical seismograms are arranged according to reduced time. In the region beyond the fault the amplitudes are diminished and the continuity of the reflected phases is lost.

The character of the wave motion about the fault can be seen best in the contoured finite difference grid of the dilatation and rotation (Figure 16). The greatest amount of disturbance is observed in the rotation. Continuity in the reflected shear is completely disrupted by a structure which in this case is approximately one wavelength high.

The refracted shear maintains its continuity but is distorted. The diffracted shear wave is dependent on the angle as indicated by the modulation of the amplitude. The compressional reflection off the face of the fault can be seen to the left of the fault. Below the interface the diffracted-reflected compressional wave dominates. Toward the left there is little evidence of generations of reflected heave wave. Toward the right the newly formed diffraction is beginning to form additional phases in the head wave. Depending on the position of the fault or faults, multiple head waves could be generated.

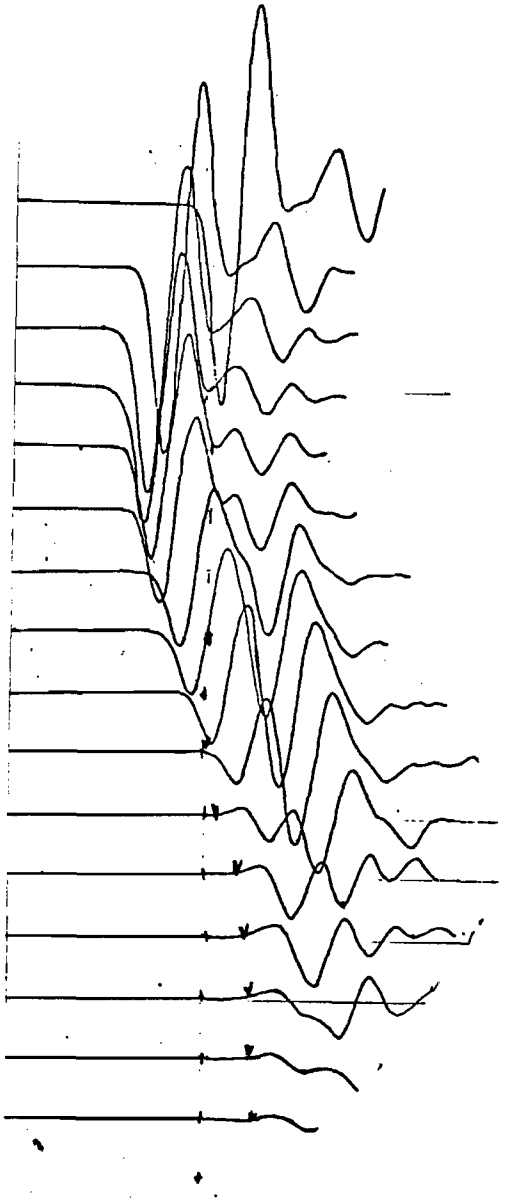

Figure 15. Vertical particle displacements for a 0.4 kilometer downward fault at 16 kilometer range. Traces are arranged according to a reduced time for 6.0 kilometer/second.

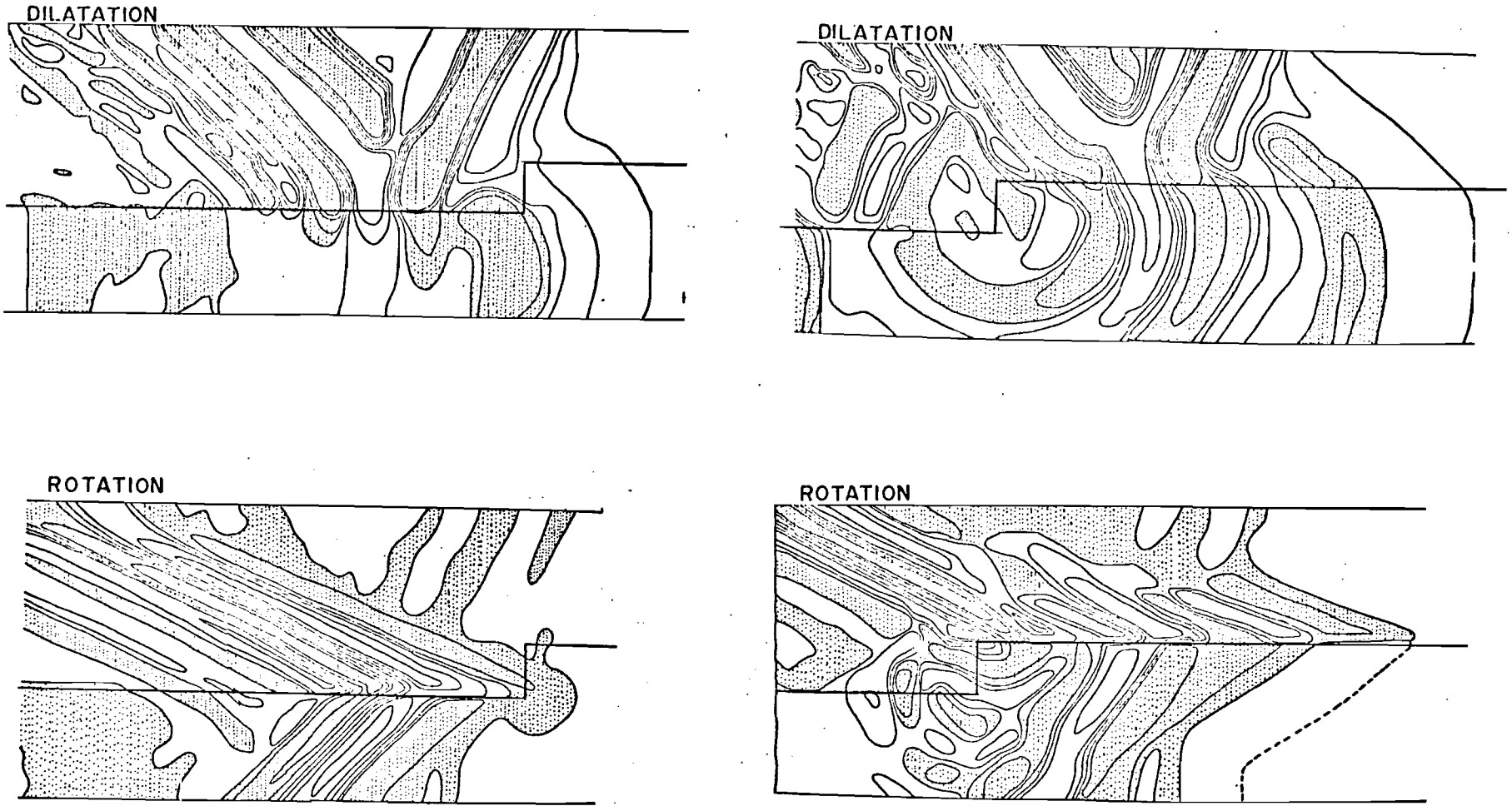

Figure 16. Dilatation and rotation contoured grid values before and after contact of head and direct waves with upward fault.

References

Alterman, Z. S. and F. Karal (1968). Propagation of elastic waves in layered media by finite difference methods, Bull. Seism. Soc. Am. 58, 367-398.

Alterman, Z. S. and D. Loewenthal (1970). Seismic waves in a quarter and three-quarter plane, Geophys. J. R. Astr. Soc. 20, 101-126.

Birch, F. (1960). The velocity of compressional waves in rocks to 10 kilobars, Part I, J. Geophys. Res. 65, 1083-1102.

Boore, D. M. (1970). Love waves in nonuniform wave guides: finite difference calculations, J. Geophys. Res. 75. 1512-1527.

Brekhovskikh, Leonid M. (1960). Waves in Layered Media, tr. by David Lieberman, Academic Press, New York.

Cagniard, L. (1962). Reflection and Refraction of Progressive Seismic Waves, tr. by E. A. Flinn and C. H. Dix, McGraw-Hill, New York.

Cerveny, Vlastislav, and Ravi Ravindra (1970). Theory of Seismic Head Waves, University of Toronto Press, Toronto.

Ewing, W. Maurice, Wenceslas S. Jardletzky and Frank Press (1957). Elastic Waves in Layered Media, McGraw-Hill, New York.

Fox, Paul J., Edward Schreiber and J. J. Peterson (1973). The geology of the oceanic crust: compressional wave velocities of oceanic rocks, J. Geophys. Res. 78, 5155-5172.

Fuchs, K. (1968). The reflection of spherical waves from transition zones with arbitrary depth-dependent elastic moduli and density, J. Phys. Earth, (Tokyo) 16, Special Issue, 27-41.

Helmberger, Donald V. (1968). The crust-mantle transition in the Bering Sea, Bull. Seism. Soc. Am. 58,179-214.

Hook, J. F. (1965). Determination of inhomogeneous media for which the vector wave equation of easticity is separable, Bull. Seism. Soc Am. 55, 975-987.

Lax, P. D. and R. D. Richtmyer (1956). Survey of the stability of linear finite difference equations, Comm. Pure Appl. Math. 9, 267-293.

Long, L. T. and Joseph W. Berg, Jr. (1969). Transmission and attenuation of the primary seismic wave, 100 to 600 km, Bull. Seism. Soc. Am. 59, 131-146.

Munasinghe, M. and G. W. Farnell (1973). Finite difference analysis of Rayleigh wave scattering at vertical discontinuities, J. Geophys. Res. 78, 2454-2466.

Musgrave, A. W. (1967). editor, Seismic Refraction Prospecting, The Society of Exploration Geophysicists, Tulsa.

Smith, T. Jefferson, John S. Steinhart and L. T. Aldrich (1966). Lake superior crustal structure, J. Geophys. Res. 71, 1141-1172.

Sokolnikoff, I. S. (1964). Tensor Analysis, John Wiley and Sons, New York.

Sommerfeld, Arnold (1964). Partial Differential Equations in Physics, (tr. by Ernst G. Straus), Academic Press, New York.

Stewart, S. W. (1968). Crustal structure in Missouri by seismic-refraction methods, Bull. Seism. Soc. Am. 58, 291-323.

Tirasawa, Tomowo and Michael J. Berry (1971). Reflected and head waves from a linear transition layer in a fluid medium, Bull. Seism. Soc. Am. 61, 1-25.

Zvolinskii, N. V. (1958). Reflected waves and head waves arising at a plane interface between two elastic media, 2, Bull. Acad. Sci. USSR, Geophys. Ser., English Transl., 1, 1-7.